# Parachutes for Planetary Entry Systems

**Juan R. Cruz**
**Exploration Systems Engineering Branch**
**NASA Langley Research Center**

V13P

# Overview

# Overview

# Introduction

# Lecture Objectives

**Provide an introduction to the design and analysis of parachutes for planetary entry systems**

- **Extensive bibliography provided for more detailed study**

**Target Audience**

- **Engineers responsible for the development and qualification of such systems**
- **Program managers and system engineers responsible for setting requirements and supervising development and qualification of such systems**

# Scope

**Lectures emphasize topics most relevant to planetary entry systems, including those for:**
- **Robotic missions**
- **Precursor human exploration missions**
- **Earth sample return missions**
- **Earth qualification of systems for planetary missions**

**Topics not emphasized are those only relevant to Earth applications**

**Topics not discussed:**
- **Parafoils, inflatable aerodynamic decelerators (IAD)**
- **Rigid aerodynamic decelerators (e.g., drag rings)**
- **Systems intended for entry or aerocapture (e.g., inflatable aeroshells)**
- **Textile impact attenuation devices (e.g., airbags)**

# Further Study I

**Bixby, H. W., Ewing, E. G., and Knacke, T. W.:  <u>Recovery Systems Design Guide</u>, AFFDL-TR-78-151, 1978.**
- Comprehensive (458 pages)
- Extensive bibliography (> 500) referenced through text
- Published in 1978 - some sections (e.g., materials) are outdated
- As with all documents, watch out for typos and incorrect information
- Required reading for engineers involved in the development and qualification of aerodynamic decelerators for planetary entry systems

**Knacke, T. W.:  <u>Parachute Recovery Systems Design Manual</u>, Para Publishing, Santa Barbara, California, 1992.**
- Comprehensive (~250 pages)
- Extensive bibliography referenced through text
- Similar to Recovery Systems Design Guide - not as comprehensive but more up-to-date
- Required reading for engineers involved in the development and qualification of aerodynamic decelerators for planetary entry systems
- Can be ordered at the following web site:  www.parapublishing.com/parachute/

# Further Study II

## H.G. Heinrich Parachute Systems Short Course
- One-week short course
- Offered on even years (next session in 2006)
- Taught by practitioners in the field with extensive practical experience
- Timed to allow time for questions during and after lectures
- Sponsored by the AIAA Aerodynamic Decelerator Systems Technology Committee
- Comprehensive
- Highly recommended for engineers involved in the development and qualification of aerodynamic decelerators for planetary entry systems
- Contact:     Dr. Jean Potvin
              Department of Physics
              Saint Louis University
              3450 Lindell Blvd.
              St. Louis, MO  63103
              314-977-8424 (voice)
              potvinj@slu.edu
              www.engr.uconn.edu/%7Eadstc/shortcourses.html

# Purposes of Aerodynamic Decelerators

**Aerodynamic decelerators typically provide one or more of the following functions:**

- **Deceleration**
- **Control acceleration**
- **Minimize descent rate**
- **Provide specified descent rate**
- **Provide stability (drogue function)**
- **System deployment (pilot function)**
- **Provide difference in ballistic coefficient for separation events**
- **Provide height**
- **Provide timeline**
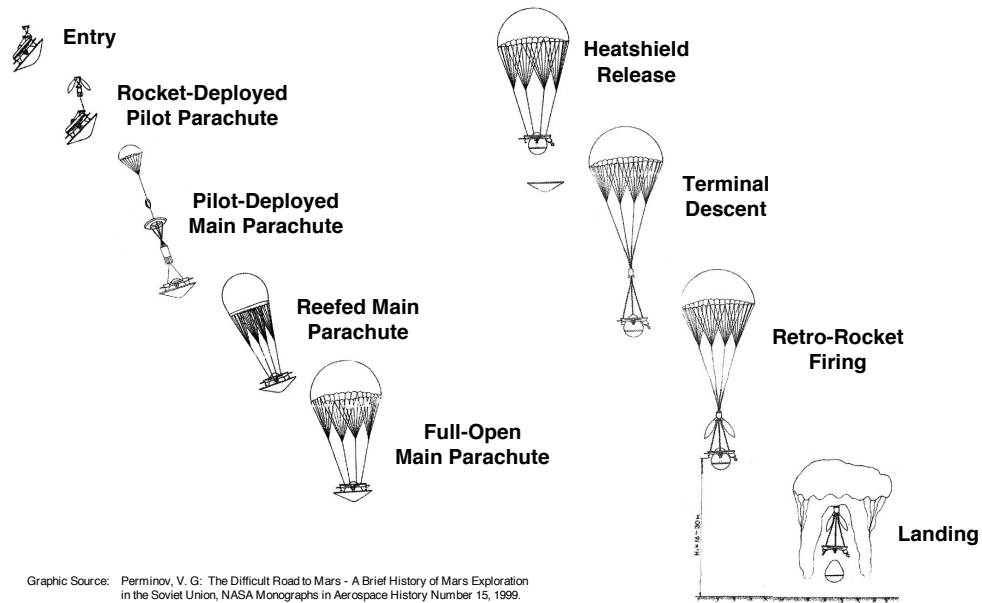- **Provide specific state (e.g., altitude, location, speed for precision landing)**
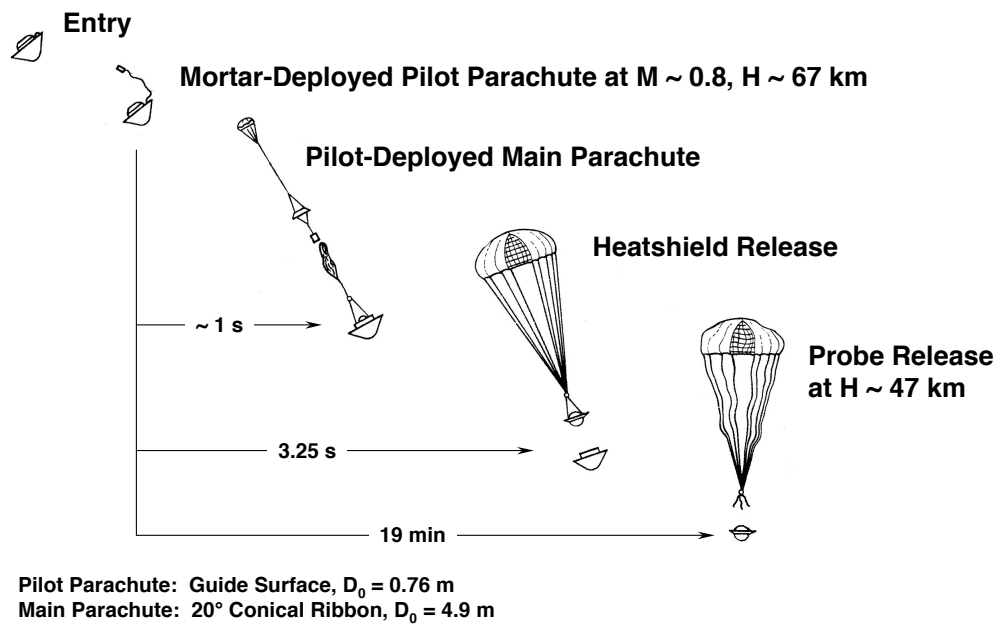
# Historical Review

## Planetary Exploration Missions Using Parachutes

| | |
|---|---|
| **Venera 5-14, USSR** | **Venus, 1969-1982** |
| **Luna 16, 20, and 24, USSR** | **Earth Sample Return from Moon, 1970-1976** |
| **Mars 2 & 3, USSR** | **Mars, 1971** |
| **Mars 6, USSR** | **Mars, 1974** |
| **Viking 1 & 2, US** | **Mars, 1976** |
| **Pioneer Venus, US** | **Venus, 1978** |
| **Vega 1 & 2, USSR** | **Venus, 1985** |
| **Galileo, US** | **Jupiter, 1995** |
| **Mars Pathfinder (MPF), US** | **Mars, 1997** |
| **Mars Polar Lander (MPL), US** | **Mars, 1999** |
| **Beagle 2, UK** | **Mars, 2003** |
| **Mars Exploration Rovers (MER), US** | **Mars, 2004** |
| **Huygens, Europe** | **Titan, 2004** |
| **Genesis, US** | **Earth Sample Return from Space, 2004** |
| **Stardust, US** | **Earth Sample Return from Comet, 2006** |

# Mars 2 & 3

**Entry**

**Rocket-Deployed Pilot Parachute**

**Pilot-Deployed Main Parachute**

**Reefed Main Parachute**

**Full-Open Main Parachute**

**Heatshield Release**

**Terminal Descent**

**Retro-Rocket Firing**

**Landing**

Graphic Source:  Perminov, V. G:  The Difficult Road to Mars - A Brief History of Mars Exploration
in the Soviet Union, NASA Monographs in Aerospace History Number 15, 1999.

# Pioneer Venus

**Entry**

**Mortar-Deployed Pilot Parachute at M ~ 0.8, H ~ 67 km**

**Pilot-Deployed Main Parachute**

**Heatshield Release**

~ 1 s

**Probe Release at H ~ 47 km**

3.25 s

19 min

**Pilot Parachute:  Guide Surface, $D_0$ = 0.76 m**
**Main Parachute:  20° Conical Ribbon, $D_0$ = 4.9 m**

Graphic Source:   Ewing, E. G., Bixby, H. W., and Knacke, T. W.:  Recovery System Design Guide, AFFDL-TR-78-151, 1978.

# Mars Pathfinder

**Entry**

**Mortar-Deployed Parachute at M = 1.7,  q = 590 Pa**

**Heatshield Separation**

**Disk-Gap-Band (DGB) Parachute**
$$D_0 = 12.7 \text{ m}$$

**Lander Separation**

**Airbag Inflation**

**Retro-Rocket Firing**

**Bridle Cut**

**Bouncing**

**Rover Deployment**

# Mars Exploration Rover EDL

# MER EDL Animation

# Genesis

Mortar-Deployed Drogue/Pilot Parachute at M ~ 1.4, H ~ 33 km

Descent Under Drogue/Pilot Parachute

Drogue/Pilot-Deployed Parafoil

Descent Under Parafoil

Mid-Air Retrieval
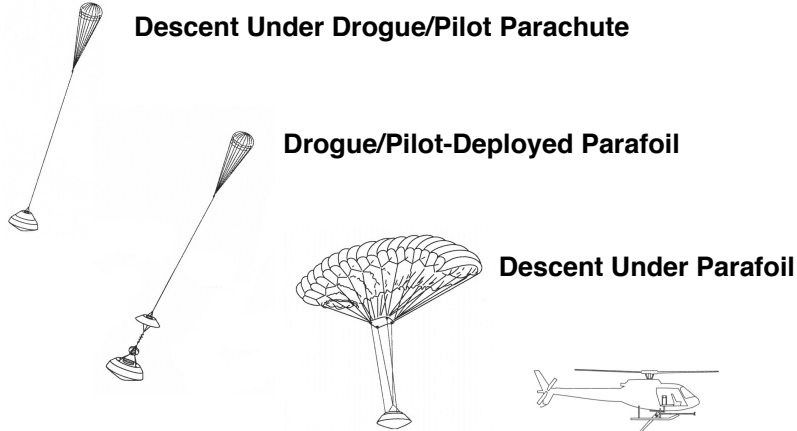
Drogue/Pilot Parachute:  DGB, $D_0$ = 2.03 m
Parafoil:  $S_0$ = 39 m$^2$

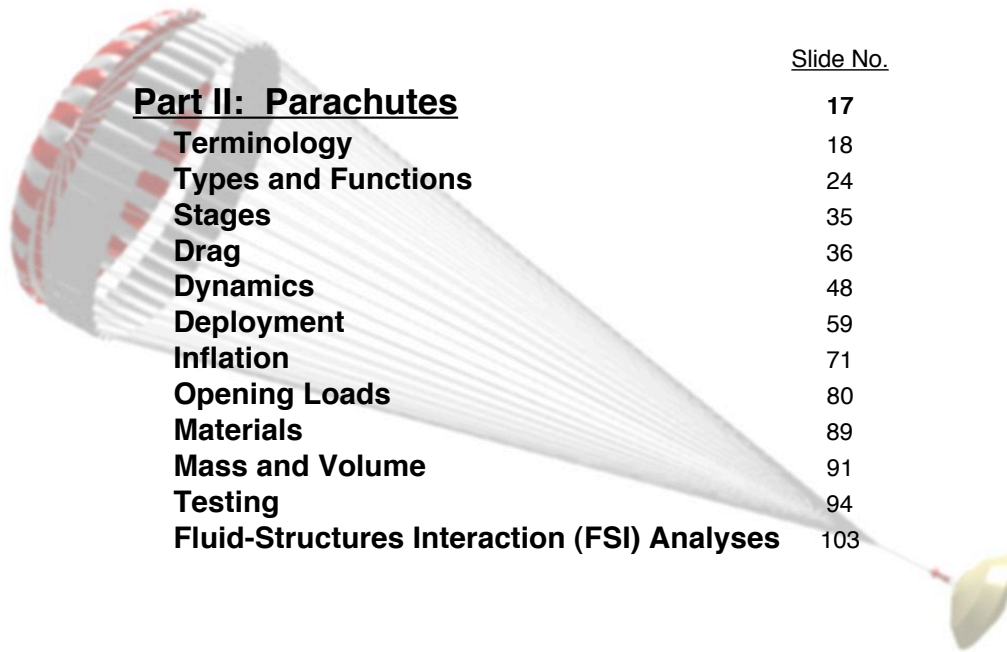Graphic Source:    Genesis Sample Return Press Kit, NASA, September  2004.

# Huygens

Entry

Mortar-Deployed Pilot Parachute at M ~ 1.5

Pilot-Deployed Main Parachute

Heatshield Separation

Descent Under Main Parachute

Main Parachute-Deployed
Drogue Parachute

Descent Under
Drogue Parachute

Touchdown

2.5 s

30 s

15 min

~ 2 hr
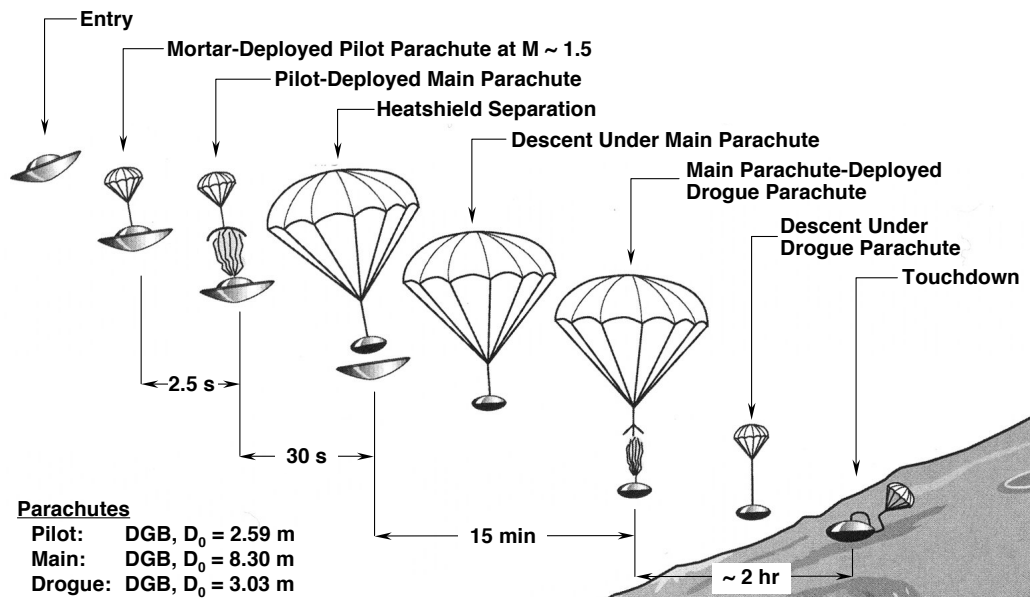
**Parachutes**
Pilot:      DGB, $D_0$ = 2.59 m
Main:     DGB, $D_0$ = 8.30 m
Drogue:  DGB, $D_0$ = 3.03 m

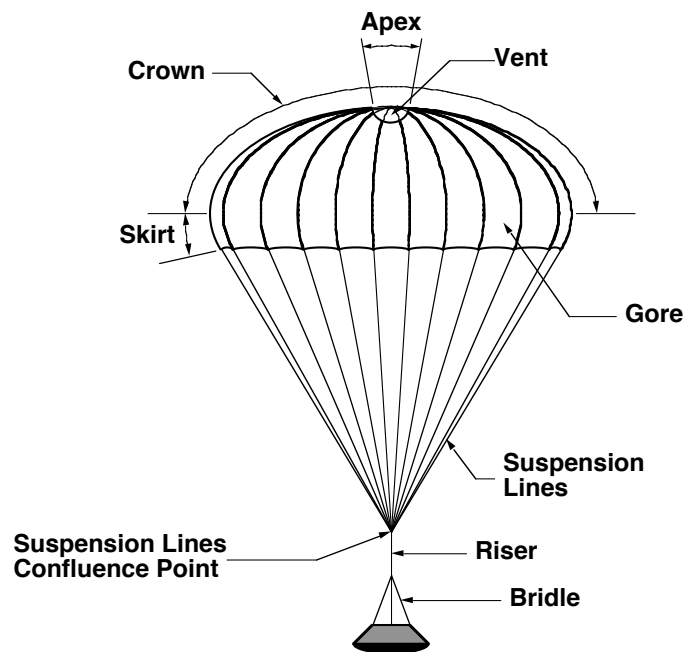Graphic Source:    Cassini-Huygens Saturn Arrival Press Kit, NASA, June 2004.

# Parachutes

Parachutes 17

# Terminology I



Parachutes:  Terminology 18

# Terminology II

<u>Nominal Area</u>, $S_0$
- **Area based on canopy constructed surface area**
- **Includes vent area and other open areas (e.g., gap area in a DGB parachute)**
- **Often (but not always!) used as reference area for aerodynamic coefficients**

<u>Nominal Diameter</u>, $D_0$
- **Fictitious diameter based on $S_0$:**

$$D_0 = \sqrt{\frac{4S_0}{\pi}}$$

- **Often (but not always!) used as reference length for aerodynamic coefficients and other calculations**

# Terminology III

<u>Constructed Diameter</u>, $D_c$
- **Maximum diameter of the parachute (measured along the gore radial seam) of the parachute**

<u>Conical Parachute Base Angle</u>, $\mu$

<u>Vent Diameter</u>, $D_v$

<u>Vent Area</u>, $S_v$
- **Constructed area of the vent**
- **Although related, the vent area and vent diameter ($D_v$) are not always related by the simple relationship between the area and diameter of a circle (see following example for a conical parachute)**
- **$S_v$ is typically ~1% of $S_0$**
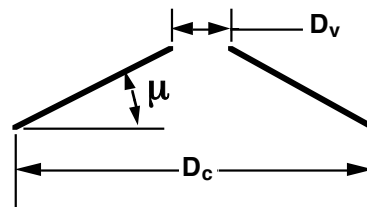
# Terminology IV

**Geometric Porosity, $\Delta_g$**
- **Ratio of total open areas (e.g., Vent Area) to the Nominal Area**
- **Usually expressed as a percentage**

**Total Porosity, $\Delta_t$**
- **The sum of the geometric porosity and an equivalent porosity due to fabric permeability**
- **Fabric permeability (i.e., flow through the fabric material) is converted to an "equivalent" open area of the parachute to determine the porosity due to fabric permeability**
- **Usually expressed as a percentage**

**The geometric and total porosity have a significant effect on the performance of the parachute (e.g., drag, stability, peak opening load). Consideration of total porosity is important in the design and testing of parachutes for planetary missions since there can be significant differences between the total porosity in an Earth test and actual flight.**

# Terminology V

**Example:  Conical Parachute**
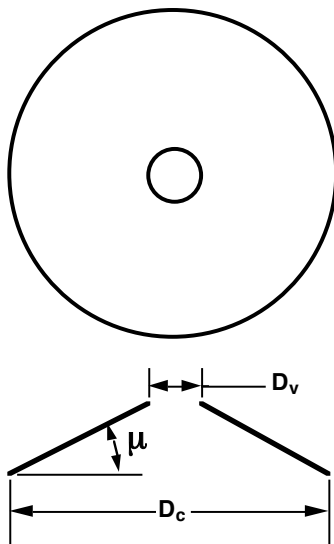


$$S_0 = \lambda\, \frac{D_c^2}{4}\, \sqrt{1+ \tan^2 \mu}$$

$$D_0 = \sqrt{\frac{4S_0}{\lambda}}$$

$$S_v = \lambda\, \frac{D_v^2}{4}\, \sqrt{1+ \tan^2 \mu}$$

$$\lambda_g = \frac{S_v}{S_0}$$

# Terminology VI

## Projected Area, $S_p$
- Projected area of the inflated parachute
- Sometimes used as reference area for aerodynamic coefficients in parachutes for which it is difficult to define $S_0$ (e.g., Guide Surface parachutes)
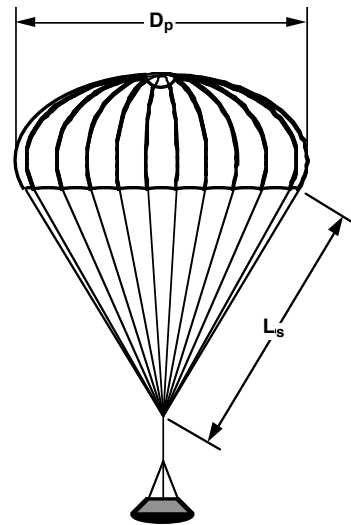
## Projected Diameter, $D_p$
- Maximum projected diameter of the parachute based on $S_p$:

$$D_P = \sqrt{\frac{4S_P}{\pi}}$$

## Suspension Line Length, $L_s$
- Typically $L_s/D_0 = 1$ to $2$

# Parachute Types

## Solid Textile Parachutes
- Parachutes with canopies fabricated mainly from cloth materials
- Typically these types of parachutes have no openings other than the vent
- Relatively easy to manufacture

**Guide Surface Parachute**

## Slotted Textile Parachutes
- Parachutes with canopies fabricated from either cloth materials or ribbons
- These types of parachutes have extensive openings through the canopy in addition to the vent
- Can be expensive to manufacture
- Most common parachute type used in planetary exploration missions

**Galileo Ribbon Parachute**
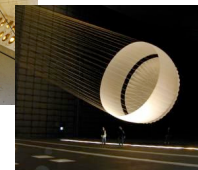
**MER DGB Parachute**

# Solid Textile Parachutes I

| Type | Constructed Shape | | $\dfrac{D_c}{D_o}$ | Inflated Shape $\dfrac{D_p}{D_o}$ | Drag Coef. $C_{D_o}$ Range | Opening Load Factor $C_x$ (Inf. Mass) | Average Angle of Oscillation | General Application |
|------|------|------|------|------|------|------|------|------|
| | Plan | Profile | | | | | | |
| Flat Circular |  | — — | 1.00 | .67 to .70 | .75 to .80 | ~1.8 | ±10° to ±40° | Descent |
| Conical |  |  | .93 to .95 | .70 | .75 to .90 | ~1.8 | ±10° to ±30° | Descent |
| Bi-Conical |  |  | .90 to .95 | .70 | .75 to .92 | ~1.8 | ±10° to ±30° | Descent |
| Tri-Conical |  |  | .90 to .95 | .70 | .80 to .96 | ~1.8 | ±10° to ±20° | Descent |
| Extended Skirt 10 % Flat |  |  | .86 | .66 to .70 | .78 to .87 | ~1.4 | ±10° to ±15° | Descent |
| Extended Skirt 14.3 % Full |  |  | .81 | .66 to .70 | .75 to .90 | ~1.4 | ±10° to ±15° | Descent |

Graphic Source: Ewing, E. G., Bixby, H. W., and Knacke, T. W.: Recovery System Design Guide, AFFDL-TR-78-151, 1978.

# Solid Textile Parachutes II

| Type | Constructed Shape | | $\dfrac{D_c}{D_o}$ | Inflated Shape $\dfrac{D_p}{D_o}$ | Drag Coef. $C_{D_o}$ Range | Opening Load Factor $C_x$ (Inf. Mass) | Average Angle of Oscillation | General Application |
|------|------|------|------|------|------|------|------|------|
| | Plan | Profile | | | | | | |
| Hemispherical |  |  | .71 | .66 | .62 to .77 | ~1.6 | ±10° to ±15° | Descent |
| Guide Surface (Ribbed) |  |  | .63 | .62 | .28 .to .42 | ~1.1 | 0° to ±2° | Stabilization Drogue |
| Guide Surface (Ribless) |  |  | .66 | .63 | .30 to .34 | ~1.4 | 0° to ±3° | Pilot, Drogue |
| Annular |  |  | 1.04 | .94 | .95 to 1.00 | ~1.4 | <±6° | Descent |
| Cross |  | — | 1.15 to 1.19 | .66 to .72 | .60 to .78 | ~1.2 | 0° to ±3° | Descent, Deceleration |

Graphic Source: Ewing, E. G., Bixby, H. W., and Knacke, T. W.: Recovery System Design Guide, AFFDL-TR-78-151, 1978.

# Slotted Textile Parachutes

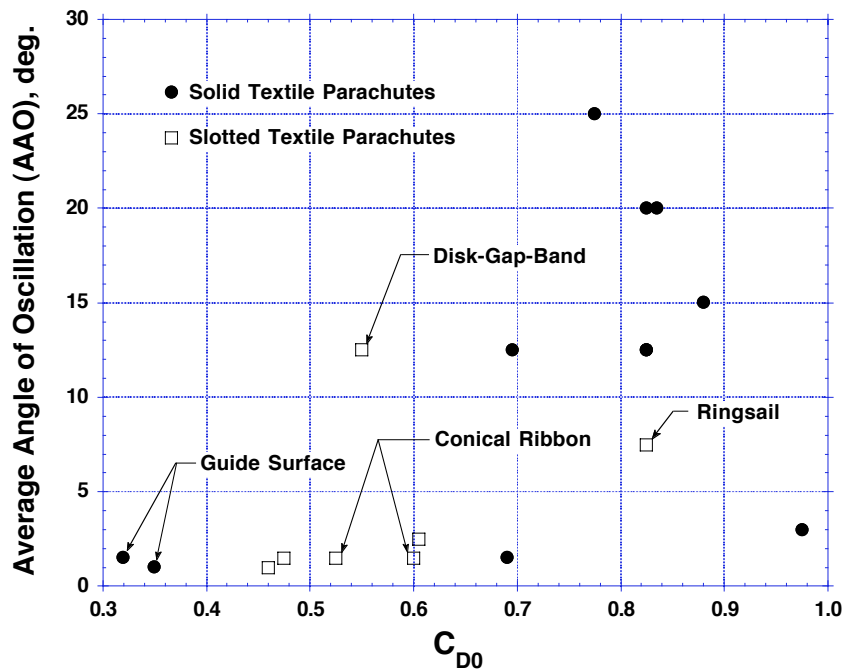| Type | Constructed Shape | | $\frac{D_c}{D_o}$ | $\frac{D_p}{D_o}$ | Drag Coef. $C_{D_o}$ Range | Opening Load Factor $C_X$ (Inf. Mass) | Average Angle of Oscillation | General Application |
|---|---|---|---|---|---|---|---|---|
| | Plan | Profile | | | | | | |
| Flat Ribbon | | | 1.00 | .67 | .45 to .50 | ~1.05 | 0° to ±3° | Drogue, Descent, Deceleration |
| Conical Ribbon | | | .95 to .97 | .70 | .50 to .55 | ~1.05 | 0° to ±3° | Descent, Deceleration |
| Conical Ribbon (Varied Porosity) | | | .97 | .70 | .55 to .65 | 1.05 to 1.30 | 0° to ±3° | Drogue, Descent, Deceleration |
| Ribbon (Hemisflo) | | | .62 | .62 | .30* to .46 | 1.00 to 1.30 | ±2° | Supersonic Drogue |
| Ringslot | | | 1.00 | .67 to .70 | .56 to .65 | ~1.05 | 0° to ±5° | Extraction, Deceleration |
| Ringsail | | | 1.16 | .69 | .75 to .90 | ~1.10 | ±5° to ±10° | Descent |
| Disc-Gap-Band | | | .73 | .65 | .52 to .58 | ~1.30 | ±10° to ±15° | Descent |

*Supersonic

Graphic Source:   Ewing, E. G., Bixby, H. W., and Knacke, T. W.:  Recovery System Design Guide, AFFDL-TR-78-151, 1978.

# Drag vs Stability Trade Space I



Average Angle of Oscillation (AAO), deg. vs $C_{D0}$

● Solid Textile Parachutes
□ Slotted Textile Parachutes

Disk-Gap-Band
Ringsail
Conical Ribbon
Guide Surface

# Drag vs Stability Trade Space II

- Graph generated by averaging $C_{D0}$ and Average Angle of Oscillation from previous tables

- General trend: increasing drag increases average angle of oscillation (decreased stability)

- Slotted textile parachutes provide better drag-stability trade space

- This chart does not address all important design trades!  Other considerations include:
  - Heritage - what data/experience do we already have?
  - Drag area vs mass trade
  - Robustness - how well will this parachute hold up in the specific application?
  - Deployment and inflation reliability
  - Cost and ease of fabrication

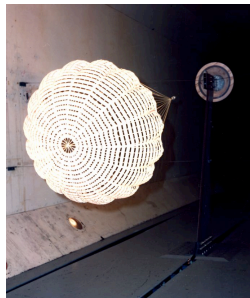*Parachute type selection is influenced by numerous considerations!*

# Canopies for Planetary Exploration Missions

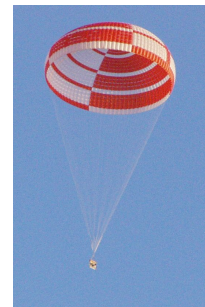**The most commonly used canopies in planetary exploration missions are:**



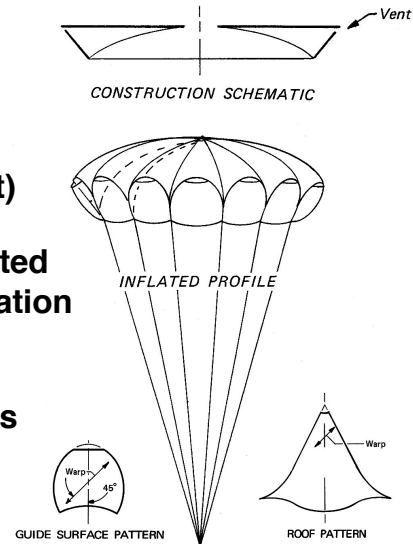**Guide Surface**



**Conical Ribbon**



**Disk-Gap-Band**



**Ringsail**

**Each of these is discussed in more detail in the following charts**

# Guide Surface (Ribless) Parachutes

- **Low drag ($C_{D0} \sim 0.3$) with good stability (0° to ±3° AAO)**

- **Used in situations where stability is principal consideration (drogue, pilot)**

- **Abrupt transition at maximum projected diameter and subsequent flow separation is reason for stability characteristics**

- **Appropriate for subsonic applications**

- **Difficult to manufacture**

- **Used by Pioneer Venus (pilot)**

*Vent*

*CONSTRUCTION SCHEMATIC*

*INFLATED PROFILE*

*Warp*

45°

*Warp*

GUIDE SURFACE PATTERN

ROOF PATTERN

Graphic Source: Ewing, E. G., Bixby, H. W., and Knacke, T. W.: Recovery System Design Guide, AFFDL-TR-78-151, 1978.

# Conical Ribbon Parachutes

- **Moderate drag ($C_{D0} \sim 0.5$) with good stability (0° to ±3° AAO)**

- **Appropriate for subsonic and supersonic applications**

- **Can be made very strong (especially if manufactured from Kevlar) and deployed at high dynamic pressure**

- **Relatively high weight per unit drag area**

- **Used by:**
    **Pioneer Venus**
    **Galileo**
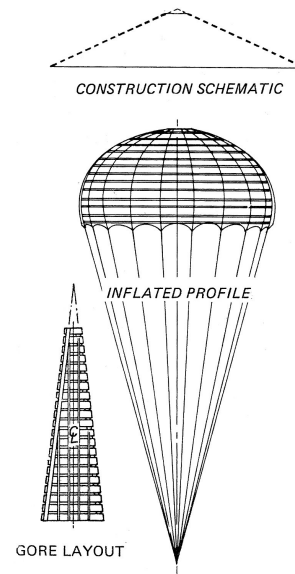
*CONSTRUCTION SCHEMATIC*

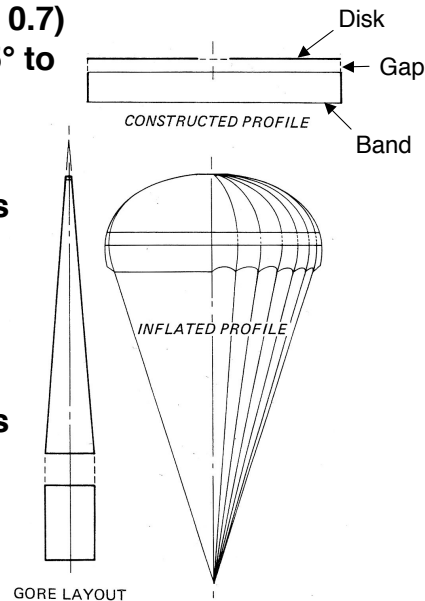*INFLATED PROFILE*

GORE LAYOUT

Graphic Source: Ewing, E. G., Bixby, H. W., and Knacke, T. W.: Recovery System Design Guide, AFFDL-TR-78-151, 1978.

# Disk-Gap-Band Parachutes

- **Low-to-moderate drag ($C_{D0} \sim 0.4$ to $0.7$) with good-to-moderate stability (±5° to ±15° AAO)**

- **Drag can be traded for stability by changing the gap and band heights**

- **Appropriate for subsonic and supersonic applications**

- **Strong heritage data at supersonic speeds in low density atmospheres key to its continued use**

- **Used by:**
  **Viking    MPF    MPL    Beagle 2**
  **MER    Huygens    Genesis**
  **Stardust**

Disk
Gap
*CONSTRUCTED PROFILE*
Band

*INFLATED PROFILE*

GORE LAYOUT

Graphic Source: Ewing, E. G., Bixby, H. W., and Knacke, T. W.: Recovery System Design Guide, AFFDL-TR-78-151, 1978.

Parachutes: Types and Functions                    33
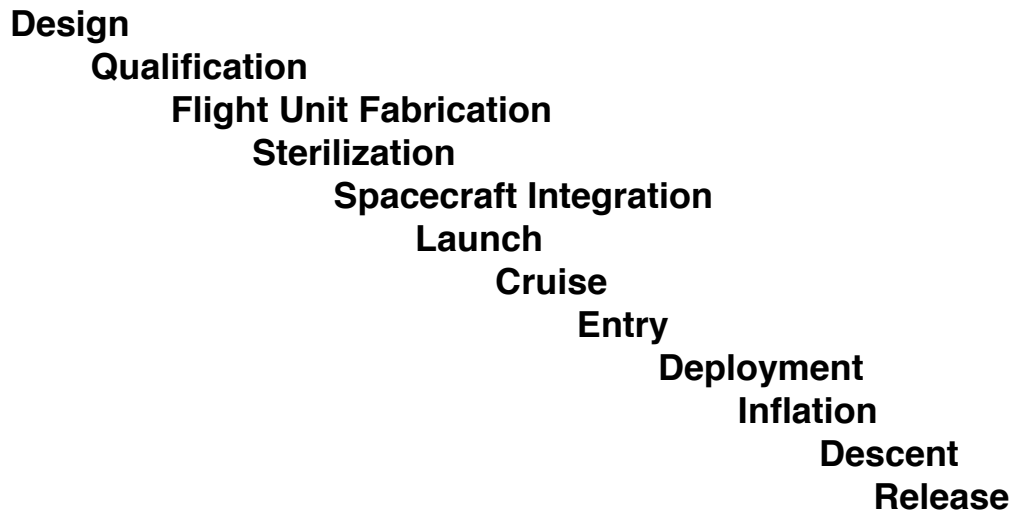
# Ringsail Parachutes

- **High drag ($C_{D0} \sim 0.8$) with good-to-moderate stability (±5° to ±10° AAO)**

- **Design tailored for optimum performance by varying canopy shape and distribution of geometric porosity throughout canopy**

- **Currently limited to subsonic applications**

- **Time consuming fabrication**

- **Relatively light weight per unit drag area**

- **Used by Beagle 2 and proposed for other missions**
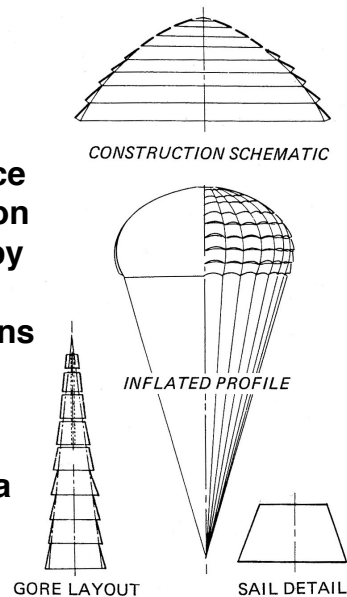
*CONSTRUCTION SCHEMATIC*

*INFLATED PROFILE*

GORE LAYOUT          SAIL DETAIL

Graphic Source: Ewing, E. G., Bixby, H. W., and Knacke, T. W.: Recovery System Design Guide, AFFDL-TR-78-151, 1978.

Parachutes: Types and Functions                    34

# Stages

**Design**
**Qualification**
**Flight Unit Fabrication**
**Sterilization**
**Spacecraft Integration**
**Launch**
**Cruise**
**Entry**
**Deployment**
**Inflation**
**Descent**
**Release**

*Each stage imposes its own set of requirements and constraints on the parachute system*

# Drag - Definition

**Drag - Force parallel to the free-stream velocity, V**

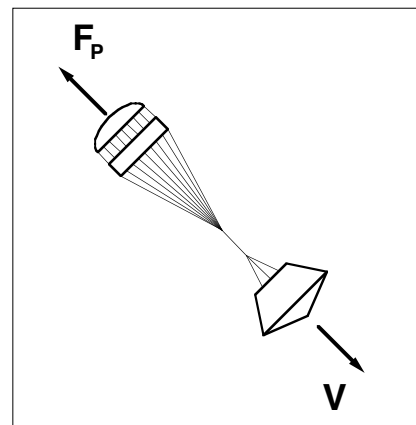**Assuming quasi steady-state conditions (e.g., parachute is fully inflated) the parachute drag force $F_P$ can be calculated from:**

$$F_P = q C_{D0} S_0$$

(using $S_0$ as reference area)

**or**

$$F_P = q C_{DP} S_P$$

(using $S_P$ as nominal area)

# C$_{D0}$

## What does C$_{D0}$ depend on?

For a <u>specific system</u> (parachute, entry vehicle) in quasi-steady conditions:

$$C_{D0} = f(M, Re, Fr, Kp, c)$$

where,

| | |
|---|---|
| Mach Number, M = V/a | Reynolds Number, Re = $\Delta$ V L/$\mu$ |
| Froude Number, Fr = V/(L g)$^{1/2}$ | Kaplun Number, Kp = k/$\Delta$ V$^2$ L |
| Effective Porosity, c = V$_\Delta$/V$^*$ | |

See "Symbols" section for a definition of all quantities used in this chart

It is difficult to match all these nondimensional quantities in a test!

The Mach Number and Effective Porosity are the most important parameters in situations involving the static aerodynamic coefficients (e.g., C$_{D0}$) of parachutes
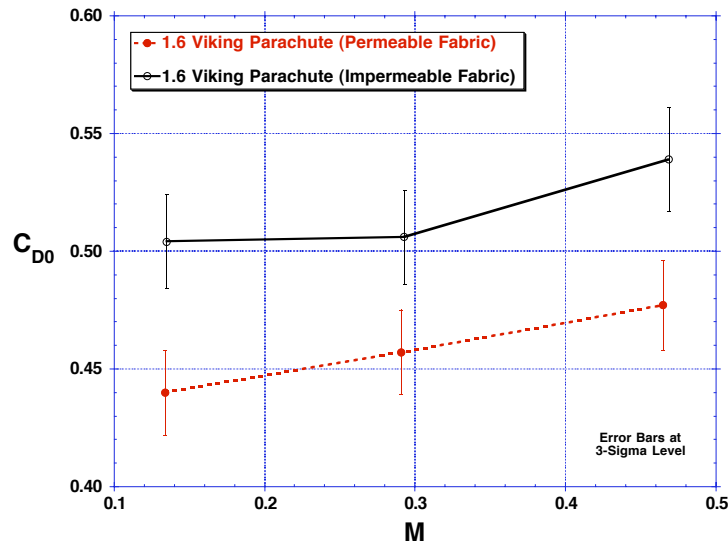
# C$_{D0}$ vs M

## Viking Parachute Wind Tunnel Test Results in Wake of Aeroshell
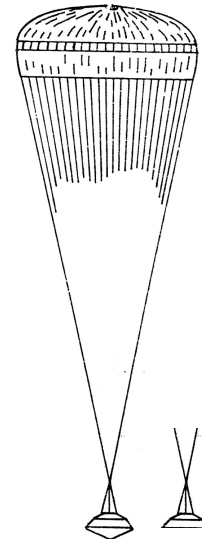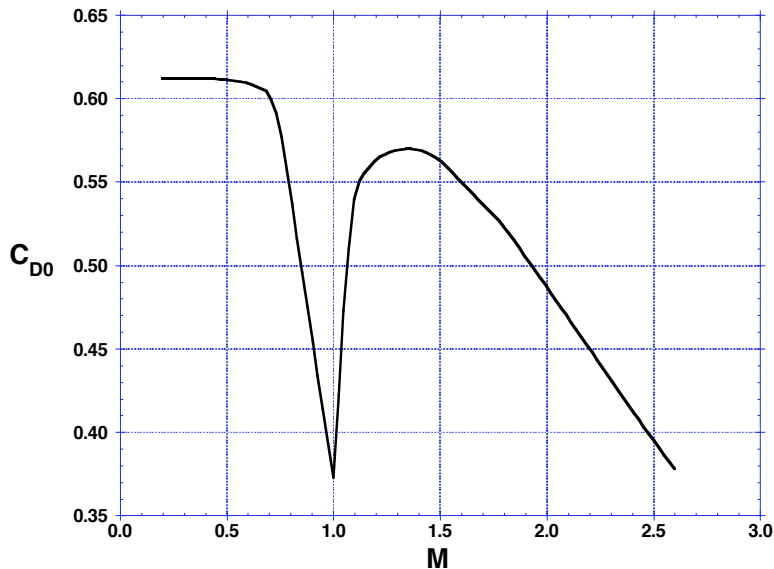


Sources:   Jaremenko, I., Steinberg, S., and Faye-Petersen, R.:  Scale Model Test Results of the Viking Parachute System at Mach Numbers from 0.1 Through 2.6, NASA CR-149377, 1971.
           Moog, R. D. and Michel, F. C.:  Balloon Launched Viking Decelerator Test Program Summary Report, NASA CR-112288, 1973.

# C$_{D0}$ vs Fabric Permeability



- - ● 1.6 Viking Parachute (Permeable Fabric)
- ○ 1.6 Viking Parachute (Impermeable Fabric)

Error Bars at 3-Sigma Level

*The effects of fabric permeability are significant in many parachute systems for planetary entry systems - they must be accounted for*

Source: Cruz, J. R., Mineck, R. E., Keller, D. F., and Bobskill, M. V: Wind Tunnel Testing of Various Disk-Gap-Band Parachutes, AIAA 2003-2129, 2003.

# Design Effects on C$_{D0}$ I
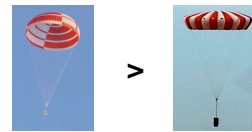
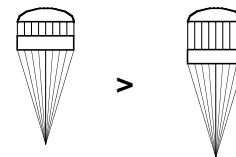**How does parachute design affect C$_{D0}$?**

C$_{D0}$ Comparison

**Canopy Type**
- **Example: Ringsail parachutes have higher C$_{D0}$ than Guide Surface parachutes**
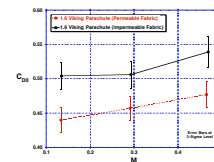


>

**Geometric Porosity**
- **Parachutes with smaller geometric porosity have a higher C$_{D0}$**
- **Example: Increasing gap size on a DGB parachute decreases C$_{D0}$**



>

**Fabric Permeability**
- **Reducing fabric permeability increases C$_{D0}$**

# Design Effects on $C_{D0}$ II

**How does parachute design affect $C_{D0}$?**

**Suspension Lines Length**
- **Increasing suspension line length increases $C_{D0}$**
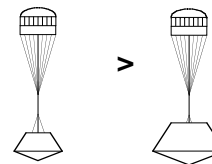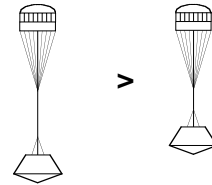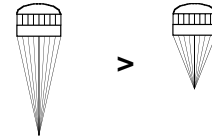
**Trailing Distance***
- **Increasing trailing distance increases $C_{D0}$**

**Forebody-to-Parachute Diameter Ratio***
- **Reducing forebody-to-parachute ratio increases $C_{D0}$**

**\*Due to wake effects of forebody on parachute**

Parachutes: Drag

41

# Wake Effects on $C_{D0}$
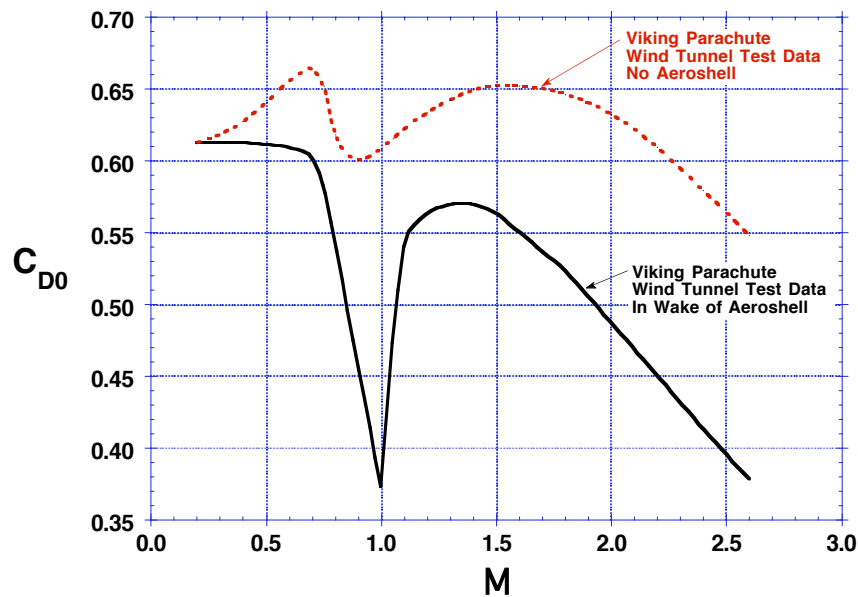


Viking Parachute
Wind Tunnel Test Data
No Aeroshell

Viking Parachute
Wind Tunnel Test Data
In Wake of Aeroshell

$C_{D0}$

M

Source:    Moog, R. D. and Michel, F. C.: Balloon Launched Viking Decelerator Test Program Summary Report, NASA CR-112288, 1973.

Parachutes: Drag

42

# How Do We Obtain $C_{D0}$?



**Re-Evaluation of Available Data**



**Flight Reconstruction**



**Wind Tunnel Testing**



**Flight Testing**

# Viking Drag Model
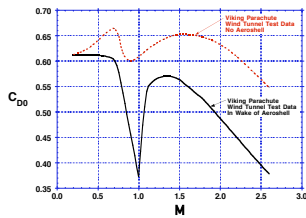


Source:    Moog, R. D. and Michel, F. C.:  Balloon Launched Viking Decelerator Test Program Summary Report, NASA CR-112288, 1973.

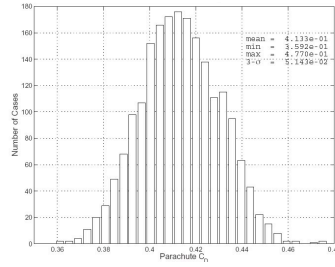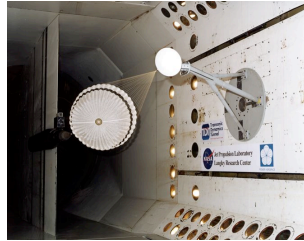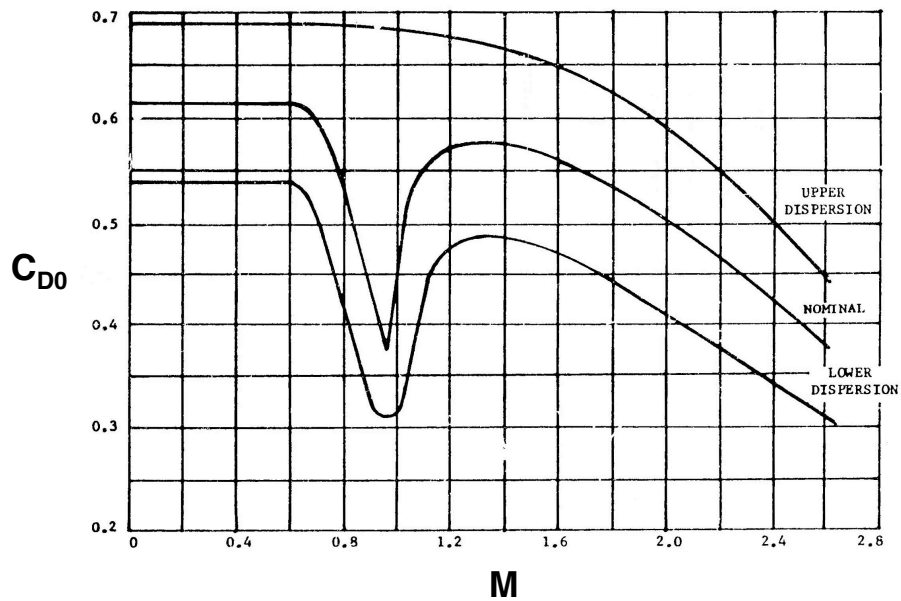# Terminal Descent Problem

**Basic Equations**

$F_P + F_{EV} = q(C_{D0}S_0 + C_{DEV}S_{EV})$

$q = \Delta\, V^2 / 2$

$F_P + F_{EV} = mg$

**Parachute Sizing - Determine $S_0$**

$C_{D0}$, $S_{EV}$, $C_{DEV}$, q, m, and g are known

$\Delta$

$S_0 = (m\, g / q - C_{DEV}S_{EV}) / C_{D0}$

**Terminal Descent Velocity - Calculate V**

$S_0$, $C_{D0}$, $S_{EV}$, $C_{DEV}$, $\Delta$, m, and g are known

$\Delta$

$V = \{2\, m\, g / [\Delta\, (C_{D0}S_0 + C_{DEV}S_{EV})]\}^{1/2}$

**Parameter Identification - Determine $C_{D0}$**

$S_0$, $S_{EV}$, $C_{DEV}$, q, m, and g are known

$\Delta$

$C_{D0} = (m\, g / q - C_{DEV}S_{EV}) / S_0$

$F_P + F_{EV}$

EV

**mg**
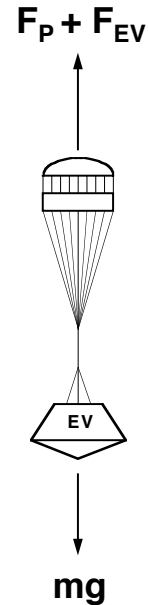
# 2 DOF Trajectory Equations

z

V

γ

$F_P + F_{EV}$

mg

x
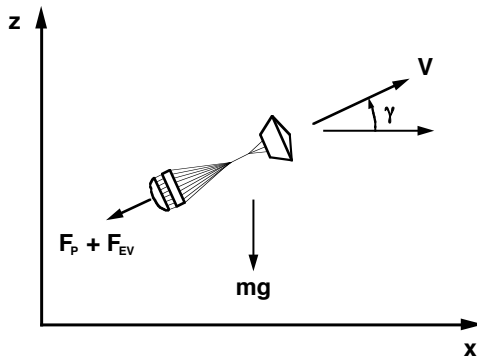
$$m\dot{V}_x = \gamma\left(F_P + F_{EV}\right)\cos\gamma$$

$$m\dot{V}_z = \gamma\left(F_P + F_{EV}\right)\sin\gamma\ \gamma\ mg$$

$$F_P + F_{EV} = q\left(C_{D0}S_0 + C_{DEV}S_{EV}\right)$$

- **These trajectory equations can be solved analytically for some simple cases**

- **In general, these equations are solved numerically**
  - **Start by transforming them into a set of first-order coupled ordinary differential equations**
  - **Solve for specified set of initial conditions**

# Parachute Clusters

**Total drag area of a parachute system can be increased by clustering parachutes**



### Advantages
- **Easier to fabricate smaller canopies**
- **Drag area can be adjusted by adding or deleting canopies**
- **Redundancy**
- **Increased stability**
- **Shorter inflation time/distance**

### Disadvantages
- **Slight loss of $C_{D0}$ (~5% for a three-canopy cluster)**
- **Problems with asynchronous inflation**
- **Heavier than a single canopy system**

# Dynamics - Importance to Planetary Missions

**Dynamic behavior of the entry system during the parachute phase of descent and landing is important for numerous reasons, for example:**

- **Scientific observations (imaging)**

- **Sensor performance (radar)**

- **Separation events (heatshield)**

- **Initial conditions for propulsive terminal descent**

- **Attitude at rocket firing events**

- **Control of horizontal velocity**



time to rocket firing = 35.90 sec
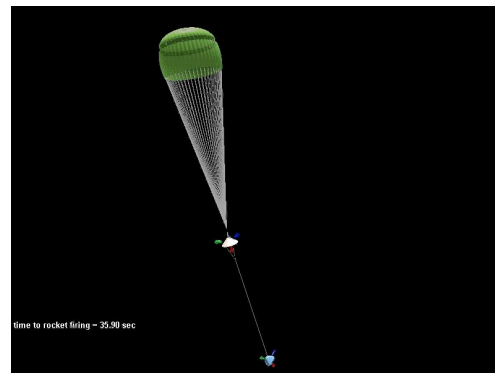
# Model for Discussion

**A simple model will be used for this discussion:**

- **Parachute and payload behave as a single unit**

- **Parachute is modeled as a rigid unit**

- **Payload generates no aerodynamic forces**

- **$\Delta$:  angle of attack;  single degree of freedom in this simplified model**

- **N:  parachute normal force acting at parachute center of pressure (CP)**

- **T:  parachute tangential force acting along axis of symmetry of parachute**

- **m:  parachute pitching moment**
  - **Shown about center of gravity, but other reference points such as suspension lines confluence point also used;  do not confuse with mass "m"**

- **Dynamic derivatives (e.g., $C_{m\alpha}$, $C_{N\alpha}$) are ignored**

---

# Static Aerodynamic Coefficients

- **$C_N$, $C_T$, $C_m$ are static aerodynamic coefficients - functions of $\Delta$**
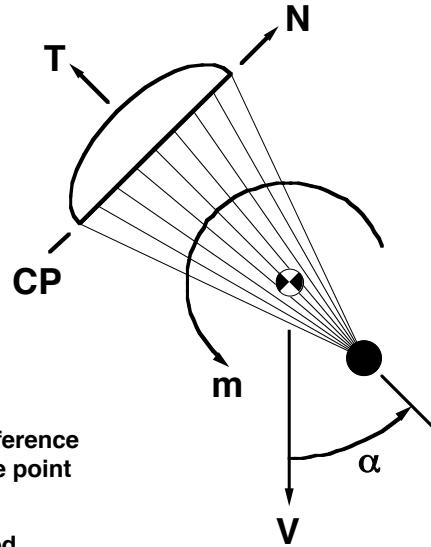
$$N = q\ S_0\ C_N \qquad T = q\ S_0\ C_T \qquad m = q\ S_0\ D_0\ C_m$$

- **$C_T \gg C_N$**

- **$C_T$ dominates drag behavior:   $C_{D0} = \sqrt{C_T^2 + C_N^2}$**

- **Center of Pressure function of $\Delta$**

    - **However, CP assumed constant in present simplified analysis**

- **Pitching moment coefficient coefficient, $C_m$, related to $C_N$**

$$C_m = -\frac{x_{CP}}{D_0}\ C_N$$

**where $x_{CP}$ is distance from CP to reference point (typically the system center of mass or suspension lines confluence point)**

- **$C_N$ and $C_m$ control stability**

# Typical $C_T$, $C_N$, and $C_m$ vs $\Delta$
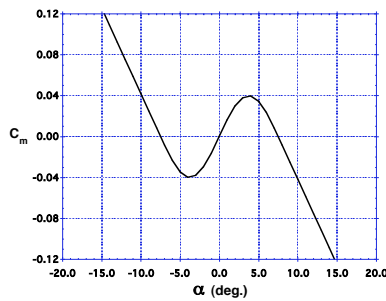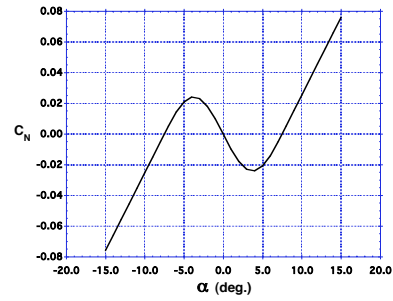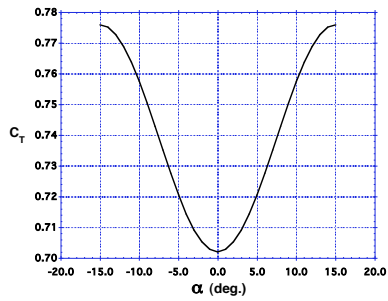
# Trim and Stability

**Trim: $C_m = 0$**

**Stable Trim Point: $dC_m/d\Delta < 0$    (restoring moment)**

**Unstable Trim Point: $dC_m/d\Delta > 0$    (diverging moment)**



Stable trim points

Unstable trim point
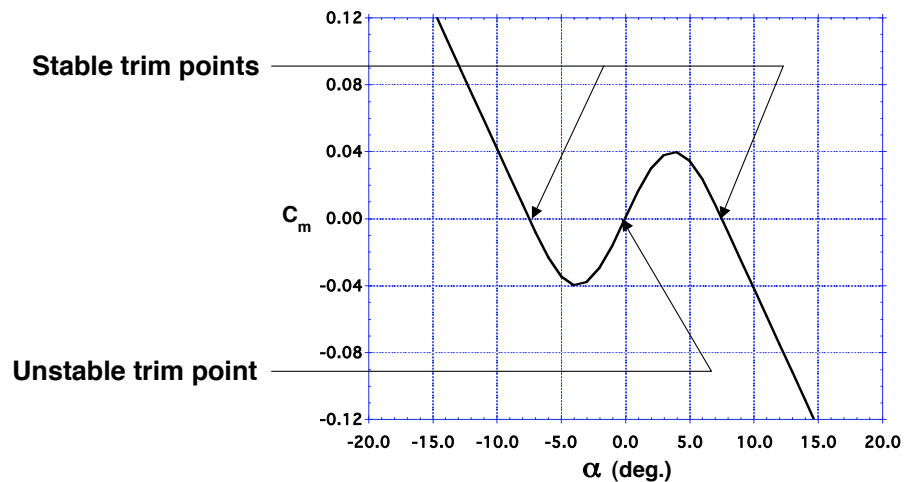
# Stable and Unstable Parachutes



"Stable Parachute"
$C_m = 0$ and $dC_m/d\Delta < 0$ at $\Delta = 0$

"Unstable Parachute"
$C_m = 0$ and $dC_m/d\Delta > 0$ at $\Delta = 0$
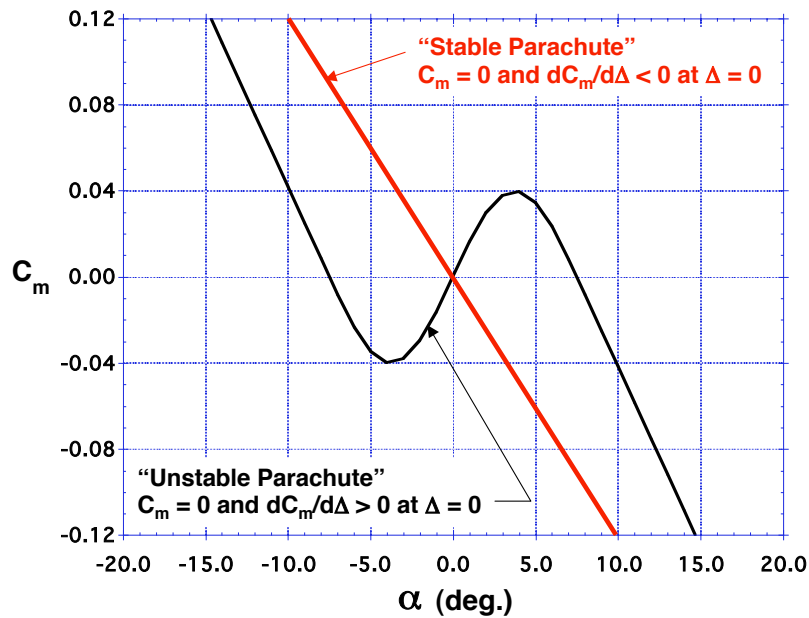
# Possible Motions

- **Gliding flight - "constant" $\Delta$**
- **Oscillation about single trim $\Delta$**
- **Oscillation from one trim $\Delta$ to another**
- **Coning**
- **Combination of the above**
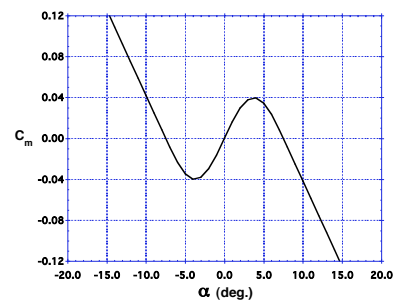


**Other factors further complicate system motions:**
- **Wind shear**
- **Unsteady wake from payload**
- **Payload dynamics**
- **Attachment to payload**
- **Parachute self induced oscillations**

# Real World Motions - Wind Tunnel Test
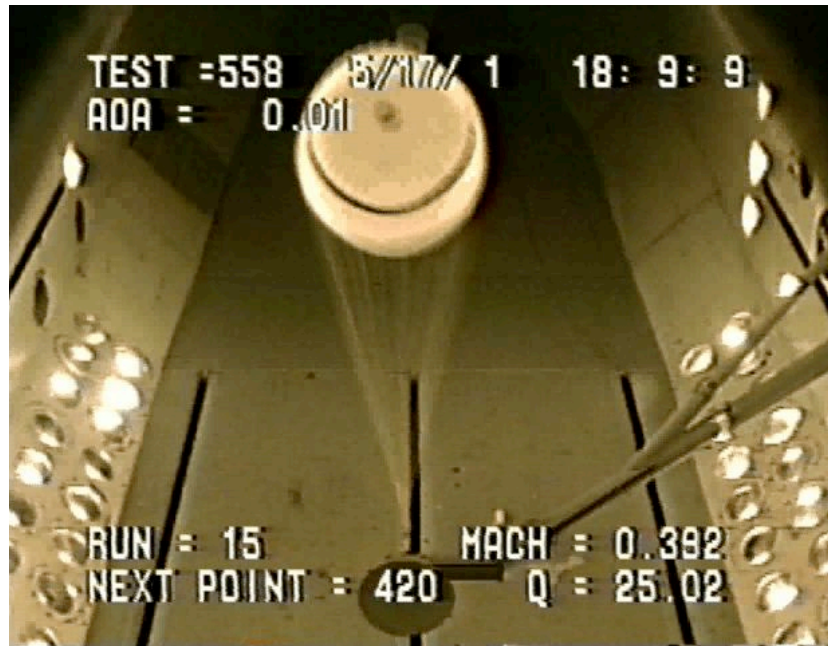
# Real World Motions - MER A Flight
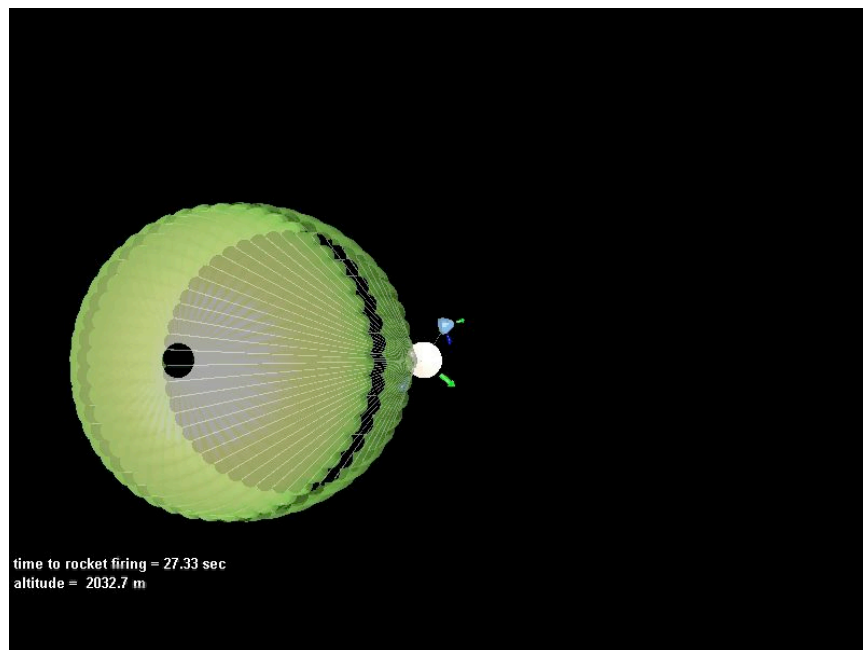
# Design Effects on Stability

**Parachute choice and design can be used to affect stability:**

- **Guide surface parachute is more stable than a Ringsail parachute**

- **Increasing band height on DGB parachutes improves stability**

- **Increasing geometric porosity improves stability**

- **Increasing fabric permeability improves stability**
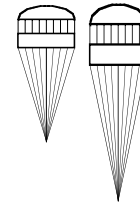
*Stability considerations may drive choice of parachute and its design*

# Multi-DOF Dynamics Models

**Complex multi-DOF dynamics models are often created to investigate stability issues**

- **Static aero coefficients**

- **Dynamic aero coefficients**

- **Physical mass and moments of inertia**

- **Apparent mass**

- **System components elasticity**
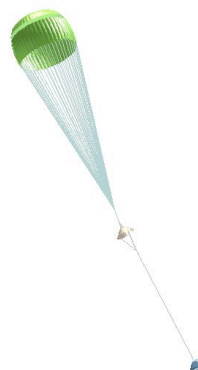
*There is still significant room for improvement in these dynamics models!*

# Deployment I

**Definition**

- **Process by which the parachute is exposed to the airstream so that inflation can start**

- **Starts with the parachute in its deployment bag within the entry vehicle**

- **Ends with the parachute stretched-out (but not inflated) and completely out of its deployment bag, streaming behind the entry vehicle**

**Deployment Methods Discussed**

- **Extractor Rocket**

- **Pilot Parachute**

- **Mortar**

# Deployment II

**A good deployment system will:**

- **Keep the parachute under tension**

- **Prevents "dumping" of the canopy (i.e., uncontrolled emergence from the deployment bag)**

- **Keep the parachute from tangling**

- **Minimize inertial deployment loads (i.e., snatch loads)**

- **Prevent significant inflation before the parachute is completely out of its deployment bag**

- **Be reliable (i.e., works every time, in the same way)**

- **Will operate properly at a variety of deployment conditions (e.g., combinations of M and q)**

- **Can be qualified through a reasonable testing program**

**Planetary parachutes use lines-first deployment systems**

# Deployment III

## Lines-First Deployment

Deployment Bag
Direction of Motion

Canopy

Suspension
Lines

Bridle & Riser

Deployment Bag

To Payload
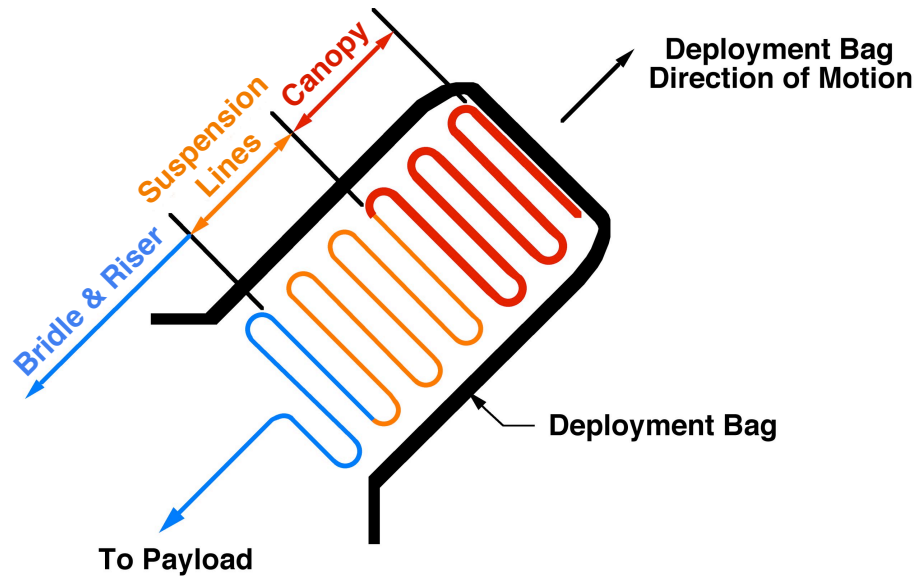
# Extractor Rocket

- **Rocket used to extract pilot or main parachute**

- **Used in Soviet Mars 2 and 3 missions**

- **Low recoil force**

- **Reliable**

- **Insensitive to deployment conditions (e.g., M and q)**

**Rocket-Deployed Pilot Parachute**

**Pilot-Deployed Main Parachute**

Graphic Source: Perminov, V. G: The Difficult Road to Mars - A Brief History of Mars Exploration in the Soviet Union, NASA Monographs in Aerospace History Number 15, 1999.

# Pilot Parachute I

## Genesis System

Mortar-Deployed Drogue/Pilot Parachute at M ~ 1.4, H ~ 33 km

Descent Under Drogue/Pilot Parachute

Drogue/Pilot-Deployed Parafoil

Descent Under Parafoil
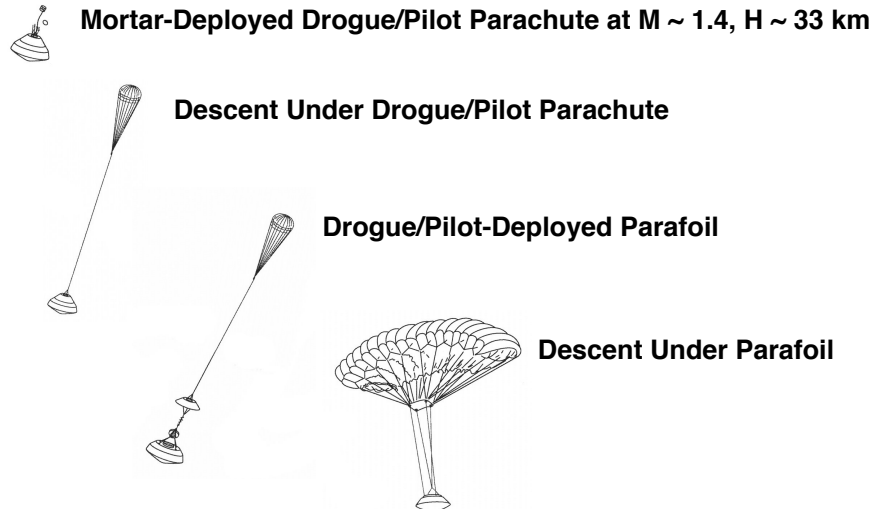
Graphic Source:   Genesis Sample Return Press Kit, NASA, September  2004.

# Pilot Parachute II

- **Used in numerous missions:**

  **Mars 2 and 3      Pioneer Venus**

  **Genesis          Stardust          Huygens**

- **Low recoil force**

- **Allows extracted parachute to be packed in almost any shape**

- **Added complexity (more than one parachute, deployment system needed for pilot parachute)**

- **May have problems with bag strip velocity**

- **May be sensitive to deployment conditions**

# Mortar I



Cover

Attachment Lugs (3)

Rails (3)

Sabot

Tube

Gas Generator
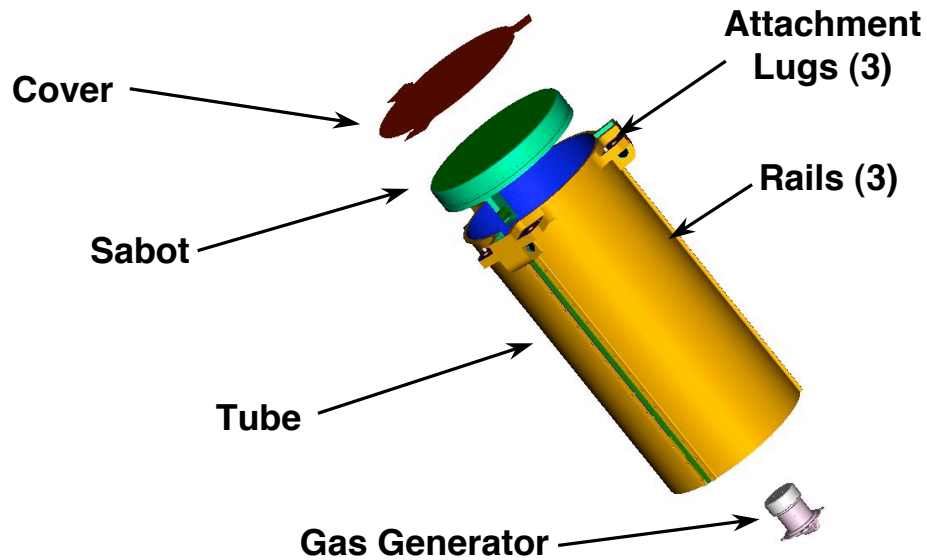
# Mortar II

- **Mortar mounted on the backshell of the entry vehicle**

- **Mortar ejects parachute pack at high velocity (100 to 130 ft/s)**

- **Parachute emerges from deployment bag in a lines-first sequence**

- **Deployment bag separates from parachute at end of deployment leaving parachute stretched-out and ready for inflation**
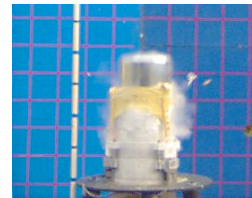
# Drop Test with Mortar Deployment
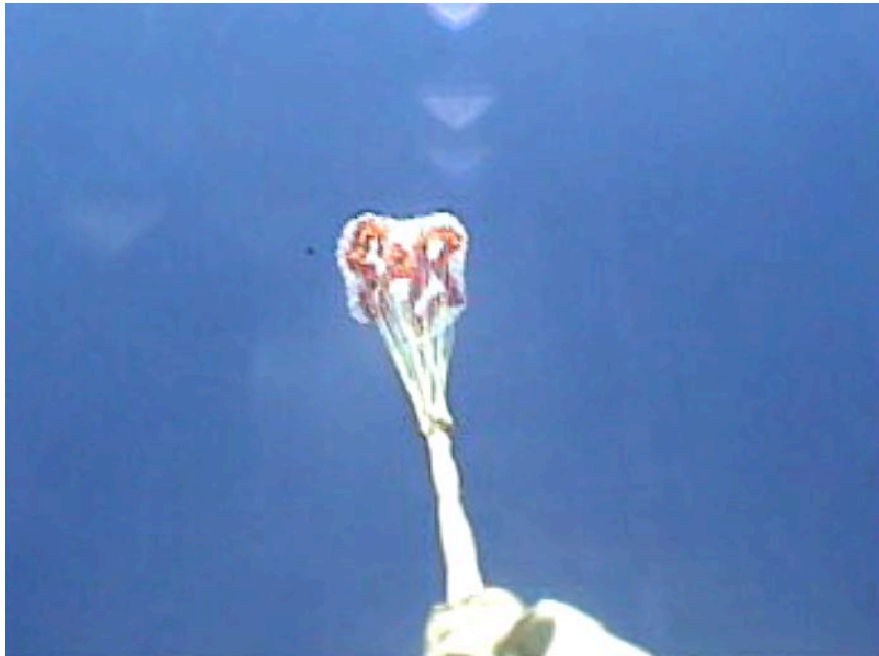
# Wind Tunnel Test with Mortar Deployment
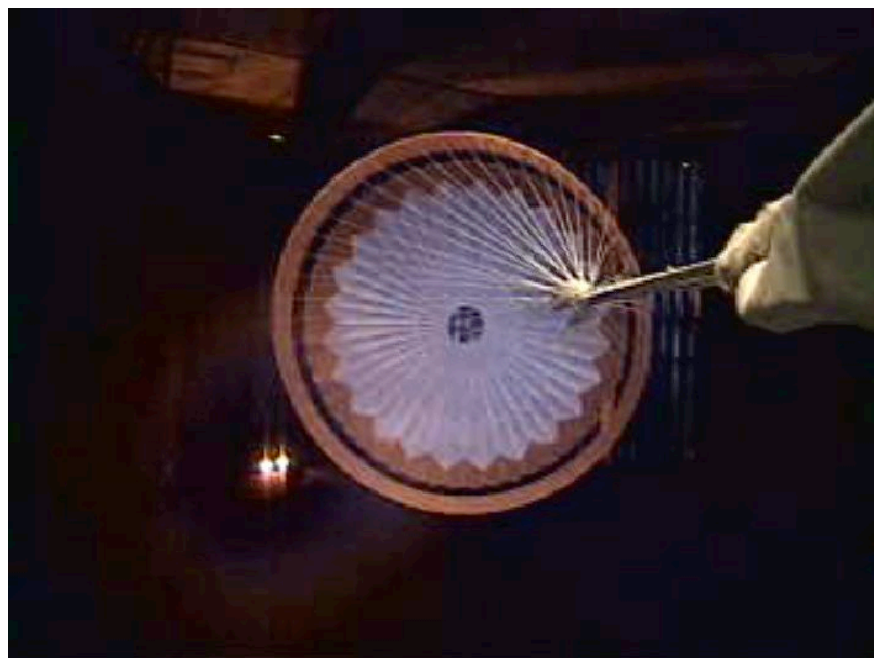
# Mortar Remarks

- Used in all US missions to Mars
- Simple and reliable
- Relatively easy to qualify
- Low bag-strip velocity
- Insensitive to deployment conditions
- High recoil force
- Parachute must be packed to high density (typically 40 to 45 lbm/ft$^3$)
- Mortar tube must be long enough to provide sufficient stroke for parachute pack acceleration
    - Parachute pack length to diameter ratio 1.0 to 2.5
- Inflexible with regards to parachute pack geometry and dimensions
    - Can be problematic wrt space allocation inside entry vehicle
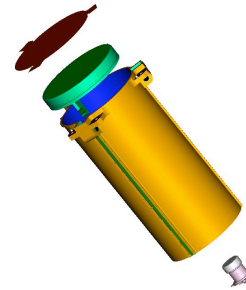
# Snatch Loads

As the parachute bag re-accelerates to the entry vehicle velocity, inertial forces are generated

These inertial forces are known as snatch loads
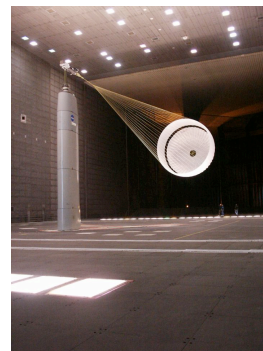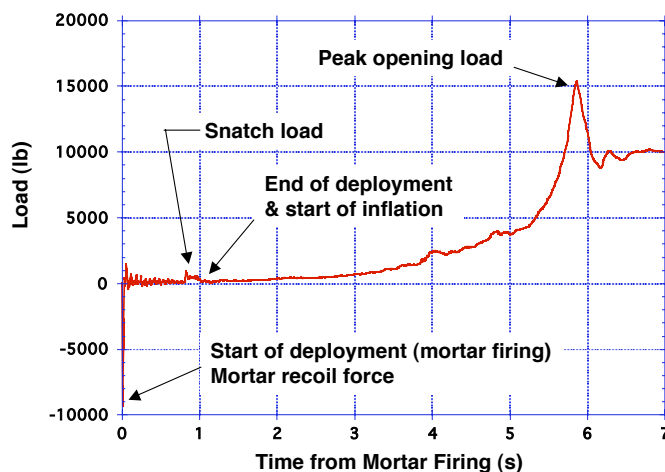
# Inflation

- **Process by which the parachute is filled (i.e., opens)**



- **Starts with the parachute stretched-out and completely out of its deployment bag, streaming behind the entry vehicle**



- **Ends with first full-inflation of the parachute**
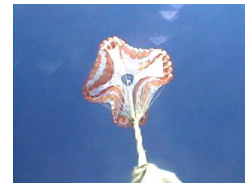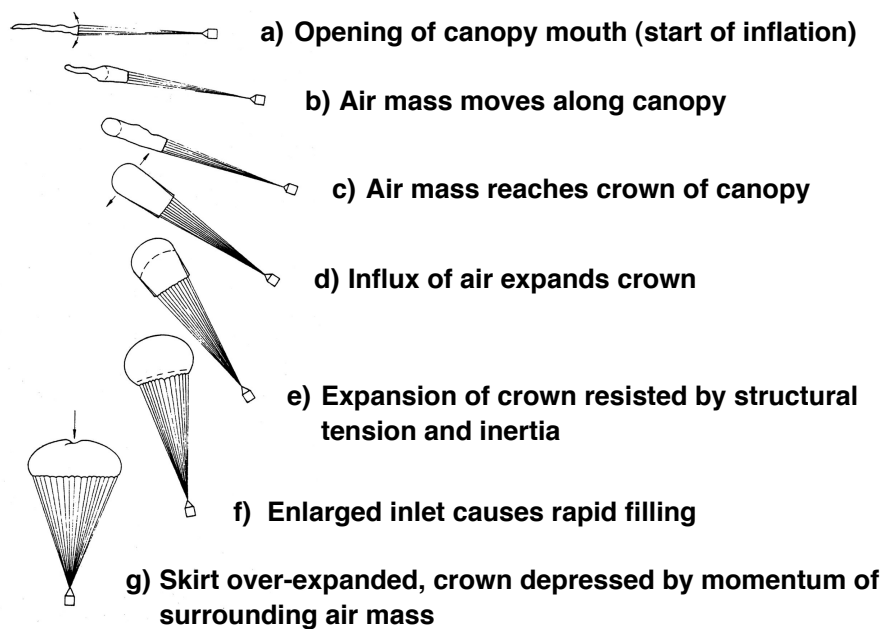
# Inflation Process



a) Opening of canopy mouth (start of inflation)

b) Air mass moves along canopy

c) Air mass reaches crown of canopy

d) Influx of air expands crown

e) Expansion of crown resisted by structural tension and inertia

f) Enlarged inlet causes rapid filling

g) Skirt over-expanded, crown depressed by momentum of surrounding air mass

Graphic Source:   Ewing, E. G., Bixby, H. W., and Knacke, T. W.:  Recovery System Design Guide, AFFDL-TR-78-151, 1978.

# Subsonic Inflation

- At subsonic speeds, inflation is often modeled as occurring over a constant number of parachute diameters (i.e., multiples of $D_0$) for a given parachute type

- Parachute is "scooping" a given volume of air to inflate

- For the most part, experimental data supports this assumption

- Thus if inflation occurs at a constant velocity, V, the inflation time, $t_{inf}$, can be estimated from:

$$t_{inf} = n_{inf} D_0 / V$$

where n depends on the parachute type and geometry (typically $n_{inf} \sim 6$ to 15)

- If V varies significantly during inflation, the equations of motion must be integrated to obtain the inflation time for a given inflation distance

# Supersonic Inflation

- At supersonic speeds, inflation is often modeled as occurring over a fixed time, proportional to the parachute diameter but independent of Mach number (in the range $1.5 \leq M \leq 2.5$)

- For the most part, experimental data supports this assumption

- Thus,

$$t_{inf} = K_{inf} D_0$$

where $K_{inf}$ depends on the parachute type and geometry (for a Viking-type DGB, $K_{inf} \sim 0.02$ s/m)

- Inflation (from bag strip to full inflation) is very fast at supersonic speeds!  For the Viking DGB with $D_0 = 16$ m, $t_{inf} \sim 0.32$ s.

# Infinite-Mass Inflation

- If inflation is of the infinite mass type  there will be little deceleration and reduction in the dynamic pressure during inflation
    - Peak opening load will occur at full inflation

- Infinite-mass inflation can happen when inflation occurs so rapidly that there is no time for significant deceleration of the entry vehicle during inflation

- Parachute inflation in thin atmospheres at supersonic speeds is often of the infinite mass type -> Mars!

- Infinite-mass inflation is difficult to obtain at subsonic speeds at low Earth altitudes - this presents a challenge to the qualification of supersonic parachutes at low Earth altitudes

- To obtain infinite-mass inflation at low Earth altitudes:
    - Payload mass must be large or,
    - Test must be conducted in a wind tunnel

# Infinite-Mass Inflation Example



**MER Drop Test - 8,000 lbm Test Vehicle**
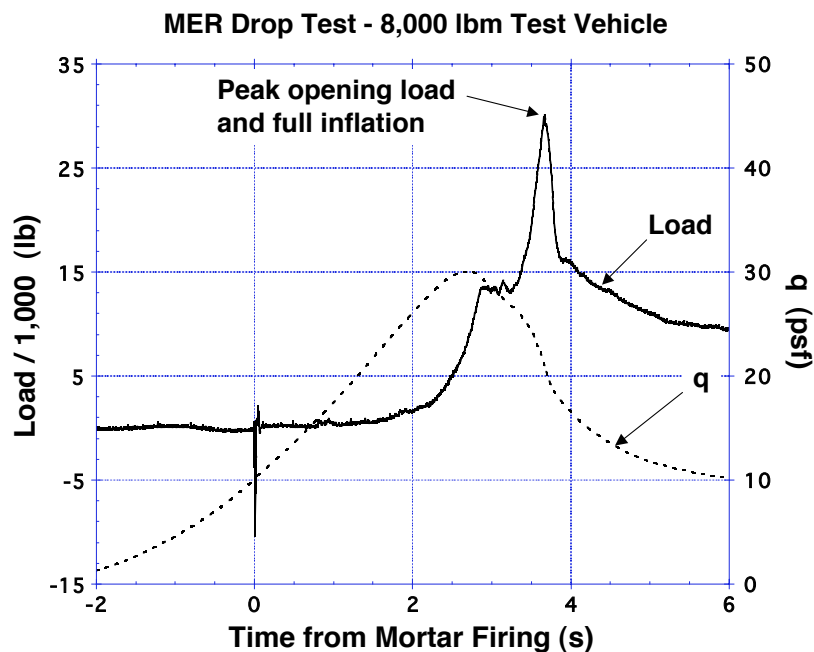
# Infinite-Mass Inflation Film
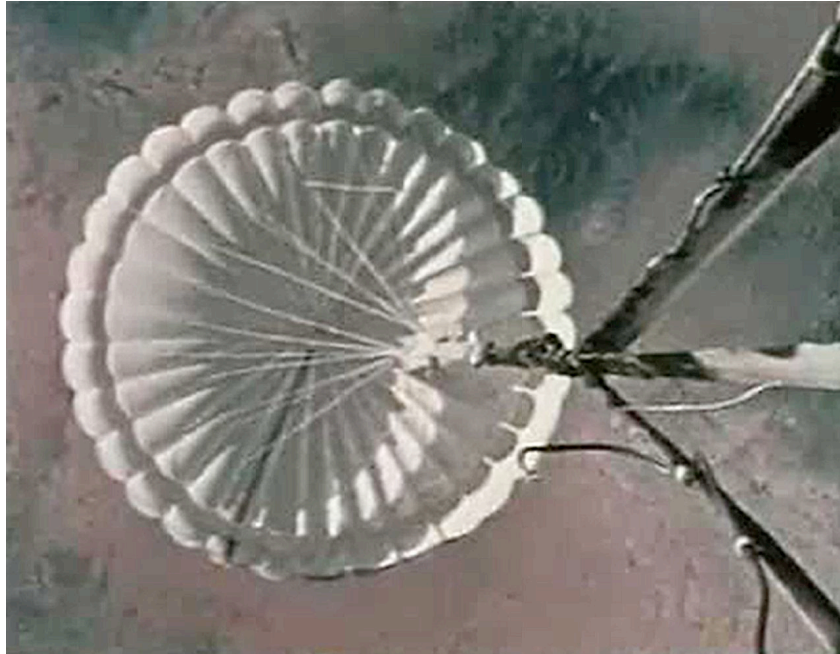
# Finite-Mass Inflation

- If the payload has "finite-mass," there will be substantial deceleration and reduction in the dynamic pressure during the inflation

    - Peak opening load <u>will not</u> occur at full inflation

- This is the typical situation when parachutes are inflated at low Earth altitudes

- It is more difficult to accurately predict the opening loads in a finite-mass inflation

# Finite-Mass Inflation Example

**MER Drop Test - 3,000 lbm Test Vehicle**
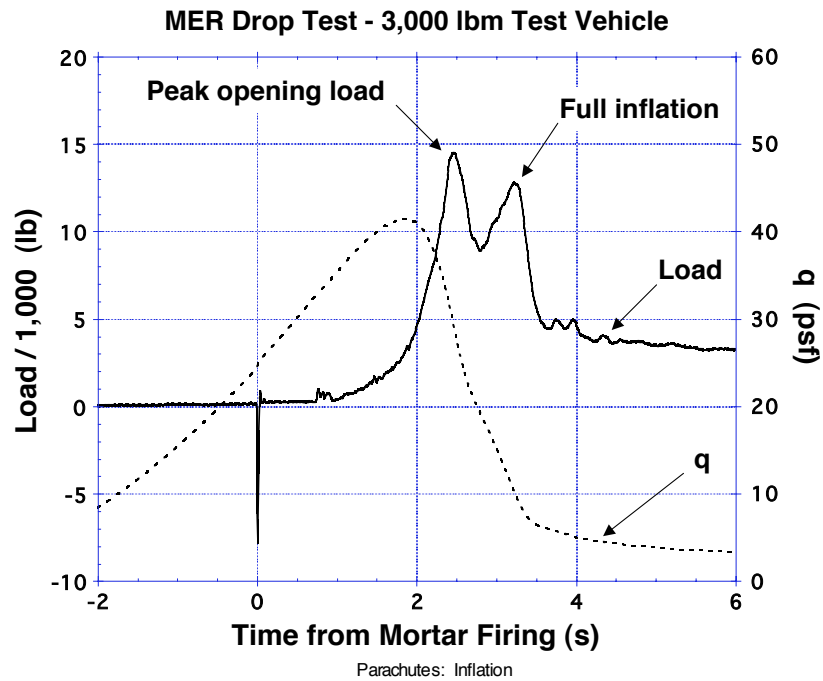
# Opening Loads

**Accurate calculation of opening loads are critical for:**
- **Stress analysis of parachute**
- **Stress analysis of entry vehicle**
- **Calculating acceleration of payload**
- **Specification of on-board accelerometers**

**Three opening loads analysis methods are discussed here:**
- **Pflanz's Method**
- **Inflation Curve Method**
- **Apparent Mass Method**

# Pflanz's Method Description

- **Simple, first-order, design book type method**

- **Requires least knowledge of the system as compared to other methods**

- **Version presented here assumes no gravity - limits application to shallow flight path angles at parachute deployment (can be extended to account for gravity and steeper flight path angles)**

- **Neglects entry vehicle drag**

- **Yields only peak opening load**

# Pflanz's Method Equations

$F_{peak} = q_1\ C_{D0}\ S_0\ C_X\ X_1$

where $X_1 = f(A, n)$ and $A = 2\ m_{EV}\ /\ C_{D0}\ S_0\ \Delta\ V_1\ t_{inf}$

**Variables definition**

$F_{peak}$ - peak opening load
$q_1$     - dynamic pressure at start of inflation
$C_{D0}$ - parachute full-open drag coefficient
$S_0$     - parachute nominal area
$C_X$     - opening load factor (from test data or tables in pages 24 through 26)
$X_1$     - force reduction factor accounting for deceleration during inflation
          (see figure 5-51 of Knacke:  Parachute Recovery Systems Design Manual)
$A$       - ballistic parameter
$n$       - inflation curve exponent (dependent on canopy type, see
          Knacke:  Parachute Recovery Systems Design Manual, p. 5-58)
$m_{EV}$ - mass of entry vehicle
$\Delta$ - atmospheric density
$V_1$     - velocity at start of inflation
$t_{inf}$ - inflation time (see inflation section for guidelines)

# Pflanz's Method Example

### MER A - Spirit

$q_1 = 729$ Pa
$C_{D0} = 0.400$ (at M = 1.75)
$D_0 = 14.1$ m
$S_0 = 156$ m$^2$
$C_X = 1.45$

$m_{EV} = 827$ kg
$\Delta = 0.00863$ kg/m$^3$
$V_1 = 411$ m/s
$t_{inf} = 0.282$ s (from previous discussion on supersonic inflation)

$A = 26.5$
$n = 2$ (for DGB parachutes)
$X_1 = 0.98$ (i.e., very close to infinite mass inflation!)

$\Delta$

$F_{peak} = 64,641$ N (within 10% of best estimate)

# Inflation Curve Method Description

- **An explicit version of Pflanz's method**

- **Assumes a drag area growth function with opening load factor**

- **Only as accurate as the assumed drag area growth function and the opening load factor**

- **Requires determination of the trajectory**

- **Easy to implement in trajectory analysis programs**

- **Yields parachute force-time history**

# Inflation Curve Method Equations

$$F_P = q C_{D0} S_0 C_X \left| \frac{t \mid t_{SI}}{t_{FI} \mid t_{SI}} \right|^n$$

$t_{FI}$

**Peak Opening Load**

$$F_P = q C_{D0} S_0$$

$$F_P = 0$$

**Parachute Force, $F_P$**

$t_{inf}$

$t_{SI}$

**Time, t**
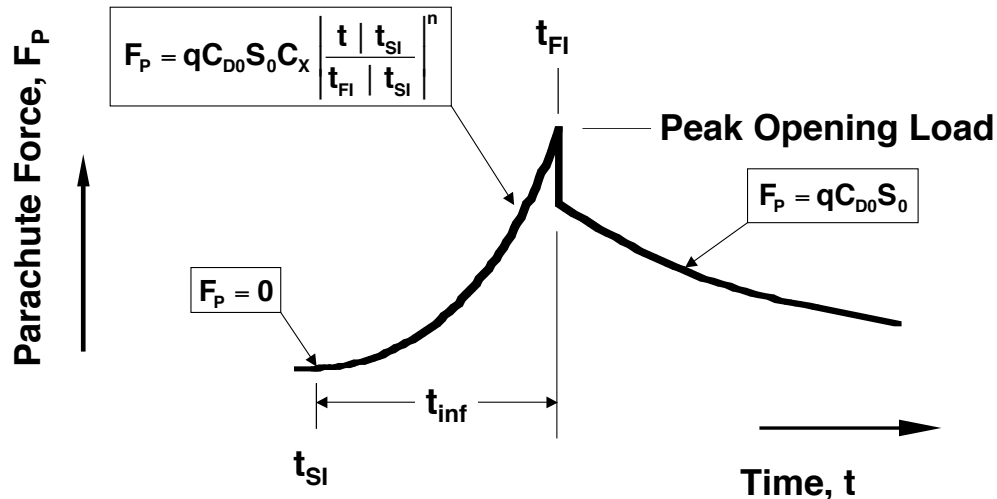
# Apparent Mass Method Description

- As the parachute inflates it carries with it a certain amount of air mass both within and around it - this air mass is known as the apparent mass

- Accelerating the apparent mass requires force, which is generated by the parachute

- Thus, the apparent mass is reflected in $F_p$, the parachute force

- The apparent mass varies with the state of the parachute during inflation

- Although apparent mass opening loads methods are more physically sound and general, they are difficult to implement due to the large number of unknowns

- Implementation in trajectory analysis is required

## Apparent Mass Method Equations

**Basic equation:**   $$F_P = qC_DS + \frac{d}{dt}\left\{(m_p + m_a)V\right\} + m_p g \sin\gamma$$

**After differentiating:**   $$F_P = qC_DS + (m_p + m_a)\frac{dV}{dt} + \frac{dm_a}{dt}V + m_p g \sin\gamma$$

$F_p$   - parachute force
$q$   - dynamic pressure
$C_DS$ - parachute drag area (function of time)
$m_a$   - apparent mass
$m_p$   - parachute mass
$V$   - velocity
$g$   - acceleration of gravity
$\Delta$   - flight path angle (positive above horizon)

**Key difficulties in implementing apparent mass opening
load methods lie in modeling $C_DS$ and $m_a$**

# Reefing

**Opening loads can be controlled by temporarily
restricting canopy at the skirt - this is known as reefing**

- **Reefing line(s) threaded through rings
  at parachute skirt**

- **Reefing line(s) length controls degree
  of reefing and drag area**

- **Reefing line is cut allowing parachute
  to continue inflation**

- **Reefing can be performed in multiple
  stages**

- **Reefing is also an effective method
  for drag area control**

- **Added complexity and possible failure
  modes need to be considered in design**
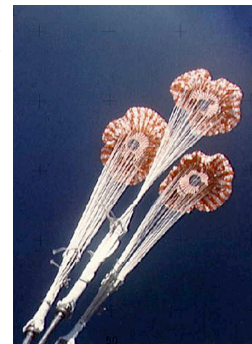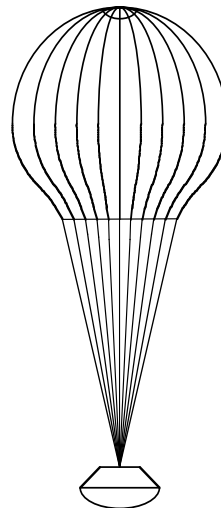
# Materials I

**Most commonly used materials for planetary parachutes:**

- **Nylon**
    - **Good strength**
    - **Often used in fabric form**
    - **480°F melting point**
    - **Poor ultraviolet light resistance**

- **Dacron**
    - **Good strength**
    - **Often used in fabric form**
    - **485°F melting point**

- **Nomex**
    - **Moderate strength**
    - **Often used in fabric form**
    - **800°F melting point**
    - **Used mainly in higher temperature applications**

*continued…*

# Materials II

- **Kevlar**
    - **High strength**
    - **Most used in lines and webbing form**
    - **850°F melting point**
    - **Poor ultraviolet light resistance**
    - **Used mainly for suspension lines, bridles, risers, and reinforcements**
    - **Has significantly reduced parachute mass as compared to the mainly-Nylon systems of the 1970's**

- **Teflon**
    - **Often used as low-friction liner for deployment bags to avoid friction burns**

- **New Materials**
    - **Spectra**
    - **Vectran**
    - **Zylon**

# Mass and Volume

**Determining the mass of a planetary parachute system can be done in various ways:**

- **Estimating mass based on historical data**

- **Bottoms-up mass estimate from system drawings**

- **Measuring weight of prototype and final systems**

# Historical Ringsail Parachute Mass Data

$$m_P / S_0 = 0.1055 \text{ kg/m}^2$$

Parachute System Mass, $m_P$ (kg)

$S_0$ (m$^2$)

Data Source: Ewing, E. G.: Ringsail Parachute Design, AFFDL-TR-72-3, 1972.
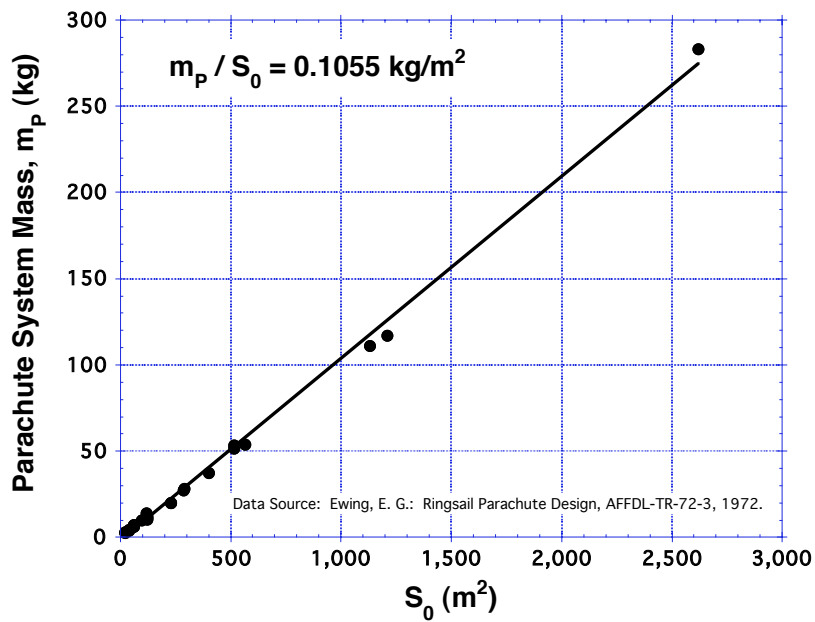
# Historical Mortar Mass Data
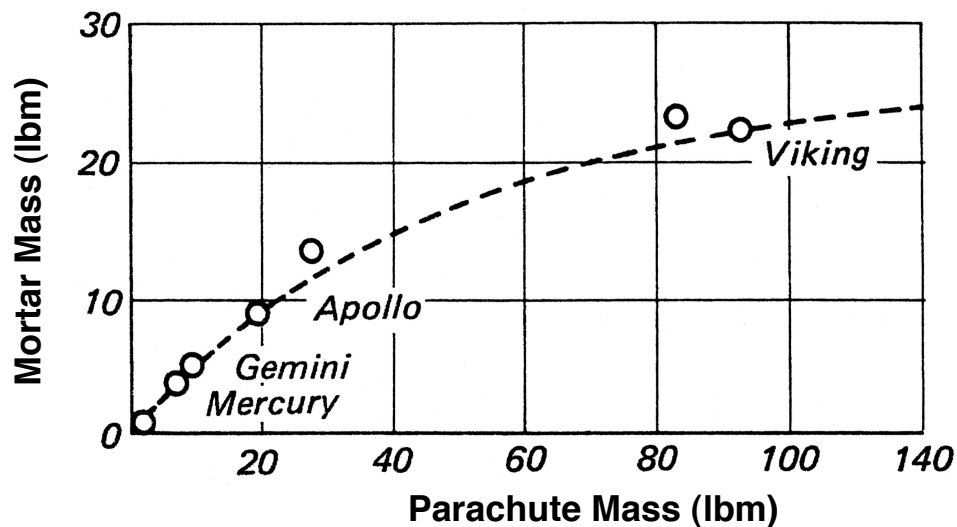
# Testing I

**Types of testing performed during a planetary parachute system design and development**

**Materials**
- **Strength & Stiffness**
- **Environmental (e.g., heat, UV, radiation, chemical)**
- **Fabric Permeability**
- **Joint and Seam**

**Wind Tunnel Testing**
- **Drag Coefficients**
- **Other Aerodynamic Coefficients**
- **Parachute Dynamics**
- **Parachute Strength**

*continued…*

# Testing II

**Flight Testing (Low- and High-Altitude)**
- **Drag Coefficient**
- **Other Aerodynamic Coefficients**
- **Parachute Dynamics**
- **Parachute Strength**
- **Deployment and Inflation**
- **System Operation and Performance**

**Ground Testing**
- **Mortar Performance**
- **Bag Strip**
- **Structural**
- **Vibration**
- **Thermal & Vacuum**

# Balloon / Rocket Flight Testing
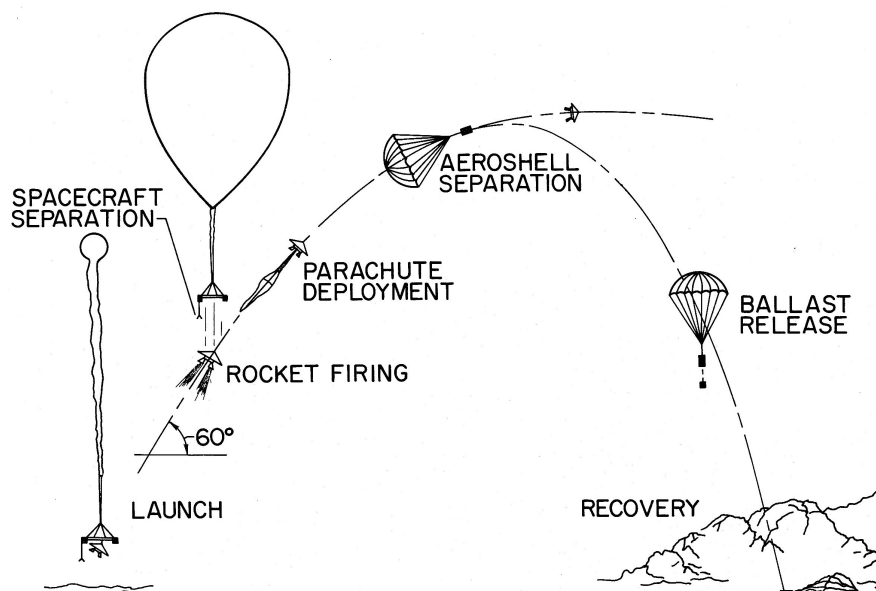


Graphic Source: Darnell, W. L., Henning, A. B., and Lundstrom, R. R.: Flight test of a 15-foot-diameter (4.6 meter) 120° conical spacecraft simulating parachute deployment in a Mars atmosphere, NASA-TN-D-4266, 1967.

# Balloon / Rocket Flight Testing Film
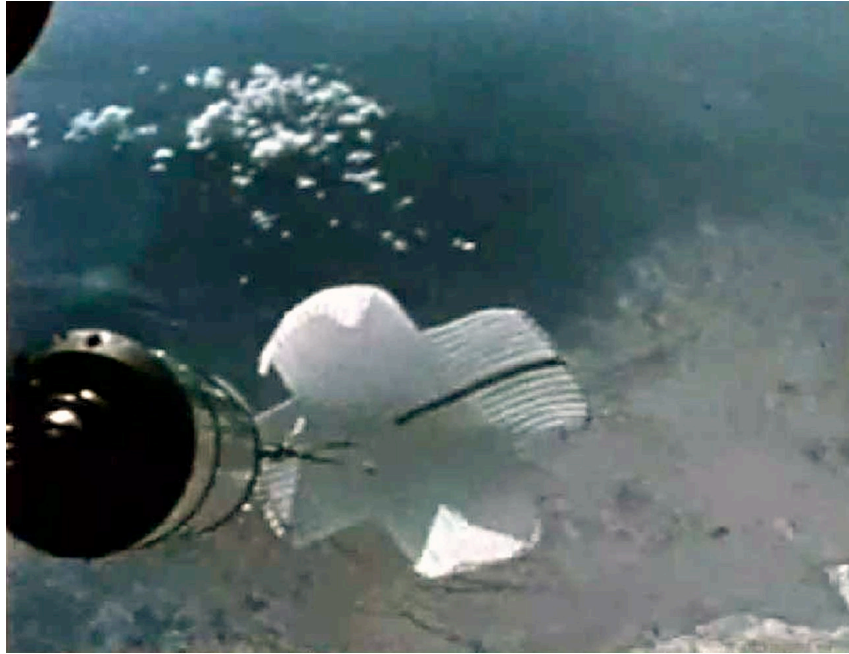


Parachutes: Testing                                                    97


# Rocket Flight Testing



L-70-258



Payload
reorientation near
flight apogee

Begin aeroshell
4.   erection at 224.50 sec

Aeroshell erection
and nose cone
5.   separation completed
at 225.18 sec

6.   Parachute
mortar firing
at 240.31 sec

3.   Vehicle separation        7.   First
at 90.08 sec                      parachute
opening
at 241.53 sec

8.   Aeroshell
separation
at 247.23 sec

2.   Maximum velocity
at ≈ 36 sec

9.   Ballast separation
at 1099.41 sec

Recruits fire at 0.3 sec

1.   Launch                          10.  Surface impact
at ≈ 1655 sec

Graphic Source:  Eckstrom, C. V. and Branscome, D. R.:  High-altitude flight test of a disk-gap-band
parachute deployed behind a bluff body at a Mach number of 2.69, NASA-TM-X-2671, 1972.

Parachutes: Testing                                                    98

# MER Low-Altitude Flight Testing

## Parachute Drag and Dynamics
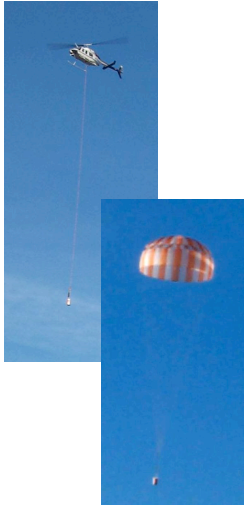
## Structural Qualification

# MER Low-Altitude Structural Qualification Flight Testing

# MER Sub-Scale Wind Tunnel Testing

## Drag Coefficient



## Aero Static
## Stability Coefficients
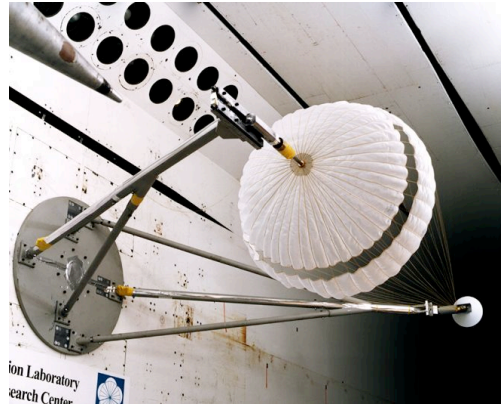
# MER Full-Scale Structural Qual Wind Tunnel Testing
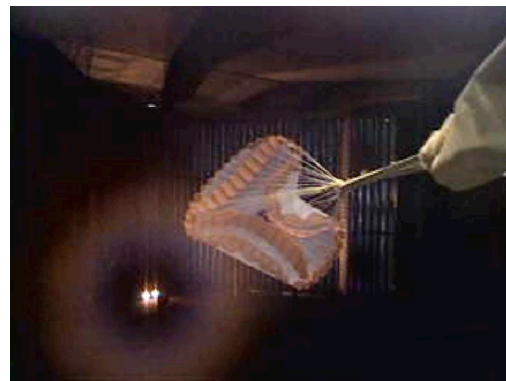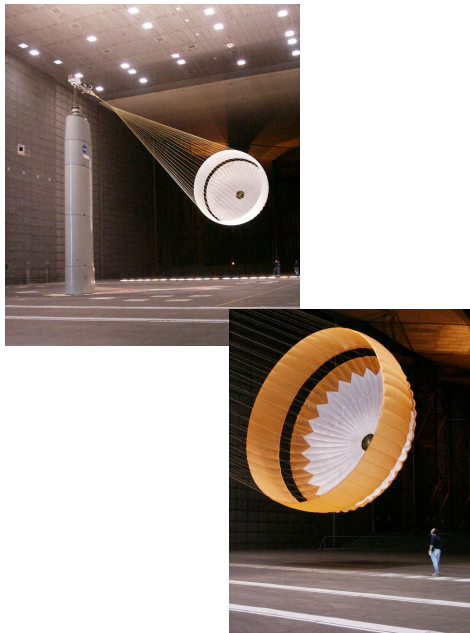
# Fluid-Structures Interaction (FSI) Analyses

- Analyses used currently to design, develop, and qualify parachutes are highly empirical - not derived from first principles

- Coupling of fluid (CFD) and structures (FEM) analyses to solve parachute problems has become viable

- CFD + FEM = FSI

- Potential benefits of FSI
    - Yield insights as to why parachutes work the way they do
    - Allow for the numerical exploration and optimization of the design before testing
    - Guide the scaling of sub-scale test results to full-scale flight
    - Guide the full-scale qualification testing of new designs
    - Expand the range of applicability of previous test results by numerical extrapolation

# Additional Materials

# Symbols

| | |
|---|---|
| $a$ | speed of sound |
| $A$ | ballistic parameter |
| $c$ | effective porosity |
| $C_{DEV}$ | drag coefficient of the entry vehicle based on $S_{EV}$ as the reference area |
| $C_{DP}$ | drag coefficient based on projected area |
| $C_D S$ | parachute drag area |
| $C_{D0}$ | drag coefficient based on nominal area |
| $C_m$ | pitching moment coefficient |
| $C_N$ | normal force coefficient |
| $C_{N\alpha}$ | derivative of $C_N$ with respect to $d\Delta/dt$ |
| $C_{m\alpha}$ | derivative of $C_m$ with respect to $d\Delta/dt$ |
| $C_T$ | tangential force coefficient |
| $C_X$ | opening load factor |
| $D_c$ | constructed diameter |
| $D_p$ | projected diameter |
| $D_v$ | vent area |
| $D_0$ | nominal diameter |
| $F_{EV}$ | drag force generated by the entry vehicle |
| $F_P$ | drag force generated by the parachute |
| $F_{peak}$ | peak opening load |
| $Fr$ | Froude number |
| $g$ | acceleration of gravity |
| $k$ | stiffness parameter |
| $K_{inf}$ | supersonic inflation constant |
| $Kp$ | Kaplun number |
| $L$ | reference length |
| $L_s$ | suspension line length |
| $H$ | altitude |

# Symbols

| | |
|---|---|
| $m$ | mass, pitching moment |
| $m_a$ | apparent mass |
| $m_{EV}$ | mass of entry vehicle |
| $m_P$ | mass of the parachute |
| $M$ | Mach number |
| $n$ | inflation curve exponent |
| $n_{inf}$ | number of nominal parachute diameters required for a subsonic inflation |
| $N$ | parachute normal force |
| $q$ | dynamic pressure |
| $q_1$ | dynamic pressure at start of inflation |
| $Re$ | Reynolds number |
| $S_{EV}$ | entry vehicle reference area |
| $S_p$ | projected area |
| $S_v$ | vent area |
| $S_0$ | nominal area |
| $t$ | time |
| $t_{FI}$ | time at full inflation |
| $t_{inf}$ | inflation time |
| $t_{SI}$ | time at start of inflation |
| $T$ | parachute tangential force |
| $V$ | velocity |
| $V_A$ | average flow-through velocity |
| $V^*$ | reference velocity $(2\,\Delta p / \Delta)^{1/2}$ |
| $V_x$ | velocity in the x direction |
| $V_z$ | velocity in the z direction |
| $V_1$ | velocity at start of inflation |
| $x, z$ | components of a Cartesian coordinate system |
| $x_{CP}$ | distance from the parachute center of pressure to the reference point |
| $X_1$ | force reduction factor |

# Symbols

| | |
|---|---|
| Δ | angle of attack |
| Δ | flight path angle (positive above horizon) |
| Δp | differential pressure across fabric |
| $\Delta_g$ | geometric porosity |
| $\Delta_t$ | total porosity |
| μ | conical parachute base angle, viscosity |
| Δ | atmospheric density |

# Acronyms

| | |
|---|---|
| AAO | Average Angle of Oscillation |
| AFFDL | Air Force Flight Dynamics Laboratory |
| AIAA | American Institute of Aeronautics and Astronautics |
| CFD | Computational Fluid Mechanics |
| CP | Center of Pressure |
| DGB | Disk-Gap-Band |
| DOF | Degree-of-Freedom |
| EDL | Entry, Descent, and Landing |
| EV | Entry Vehicle |
| FEM | Finite Element Method |
| FSI | Fluid Structures Interaction |
| IAD | Inflatable Aerodynamic Decelerator |
| MER | Mars Exploration Rovers |
| MPF | Mars Pathfinder |
| MPL | Mars Polar Lander |
| NASA | National Aeronautics and Space Administration |
| NA&SD | NASA Aeronautics and Space Database |
| UV | Ultraviolet light |

# Glossary

**Aerocapture** – an orbit insertion maneuver in which the drag generated by an entry vehicle as it flies through the atmosphere of a planet or moon is used to reduce the entry vehicle's kinetic energy so that it is captured into orbit.

**Aerodynamic Decelerator** – a device that uses drag to dissipate a payload's kinetic energy and velocity.

**Aeroshell** – an enclosure that protects a payload from the rigors of entry.

**Airbag** – an inflatable textile bag used to cushion the impact of a payload.

**Angle of Attack** – in two dimensions, the angle between the longitudinal axis of an entry vehicle or parachute and its velocity through a fluid.

**Angle of Oscillation** – the angular displacement of a parachute's axis of symmetry from the vertical or direction of travel.

**Apex** – the furthest downstream (i.e., top) portion of a parachute.

**Apparent Mass** – the mass of fluid, both within and around a parachute canopy, affected by the parachute. The apparent mass has an influence on the forces and moments generated by the parachute.

**Apparent Mass Method** – a method of calculating parachute opening loads that incorporates the effects of apparent mass.

**Backshell** – the downstream facing portion of an aeroshell.

**Bag-Strip Velocity** – the relative velocity between the parachute and the deployment bag during deployment.

**Ballistic Coefficient** – the ratio of mass to drag area of an entry vehicle or other component (e.g., heatshield).

**Ballute** – a type of aerodynamic decelerator consisting of an inflatable structure that is either attached to the entry vehicle through one or more risers (i.e., a trailing ballute) or is directly attached around the edges of the entry vehicle (i.e., an attached ballute). The inflating fluid can be provided by either a gas generator or by capturing a portion of the airflow (i.e., a ram-air ballute). The term ballute is a combination of balloon and parachute. Ballutes are also sometimes referred to as inflatable aerodynamic decelerators (IAD). Ballutes have been proposed for a variety of purposes from entry to supersonic deceleration. I discourage the use of the term ballute since it is applied to a wide variety of disparate devices. I recommend using the term *inflatable*

*aeroshell* to describe devices that are deployed and inflated prior to entry and must withstand the heat of entry, and *inflatable aerodynamic decelerator* for devices deployed and inflated at Mach numbers of five or less.

**Band** – the component of a Disk-Gap-Band parachute whose constructed shape consists of a (fabric) cylinder.  The upstream edge of the band is the skirt of a Disk-Gap-Band parachute.

**Bridle** – a multiple-leg textile component used to attach the parachute to the payload.

**Canopy** – the main drag producing portion of a parachute.

**Cluster** – an arrangement of parachutes in which two or more identical canopies are used simultaneously.

**Conical Ribbon Parachute** – a type of slotted textile parachute with a conical constructed shape consisting of ribbons in the circumferential and radial directions.

**Coning** – one possible motion of a parachute/payload system in which both the parachute and the payload rotate in circles and the combination traces two cones.

**Constructed Diameter** – the diameter of a parachute when it is held in its constructed shape (e.g., the base diameter of the cone describing the constructed shape of a conical parachute, the diameter of the hemisphere describing the constructed shape of a hemispherical parachute).

**Crown** – the top portion of a parachute canopy from its maximum diameter to the apex.

**Deployment** – the process by which a parachute is exposed to the airstream so that inflation can start.  Deployment starts with the parachute in its deployment bag and ends with the parachute completely out of its deployment bag and stretched-out (but not inflated) while streaming behind the entry vehicle.

**Deployment Bag** – a bag containing the parachute whose main purpose is that of effecting an organized deployment.

**Disk** – the component of a Disk-Gap-Band parachute whose constructed shape consists of a circular (fabric) disk.

**Disk-Gap-Band Parachute** – a type of slotted textile parachute whose constructed shape consists of a flat disk and a cylindrical band with a gap between the disk and the band.

**Drag** – the component of aerodynamic force parallel to the airstream generated by a body such as a parachute or entry vehicle.

**Drag Coefficient** – a nondimensional quantity defined as the drag of a body divided by its reference area and dynamic pressure.

**Drogue Parachute** – a parachute whose main purpose is to stabilize the payload.

**Dumping** – uncontrolled and/or unorganized emergence of a parachute from its deployment bag.

**Dynamic Pressure** – one-half the product of fluid density times the airspeed squared.

**Effective Porosity** – a measure of canopy porosity due to fabric permeability.

**Extractor Rocket** – a deployment system in which the deployment bag and parachute are pulled away from the vehicle by means of a rocket.

**Finite-Mass Inflation** – an inflation of a parachute occurring such that the change in dynamic pressure is relatively large during inflation. For a parachute, the peak opening load will often occur before full inflation during a finite-mass inflation. The term finite-mass inflation arises from the observation that if a payload's mass is low (in a constant atmospheric density, gravity-free environment) the dynamic pressure will drop significantly during inflation since the drag of the parachute will decelerate the payload. See *infinite-mass inflation* for the converse situation.

**Forebody** – a body suspended in front of a parachute.

**Froude Number** – a nondimensional number expressing the ratio of inertial to gravity forces.

**Gap** – the open portion of a Disk-Gap-Band parachute whose constructed shape consists of a cylinder joining the disk to the band by means of suspension lines.

**Gas Generator** – a pyrotechnic device that creates gas at high pressure behind the sabot of a mortar to eject the parachute in its deployment bag. Also, a pyrotechnic device that creates gas to inflate an airbag, an inflatable aeroshell, or an inflatable aerodynamic decelerator.

**Geometric Porosity** – the ratio of open areas in a parachute's canopy to the nominal area. Usually expressed in percentage.

**Gliding** – one possible motion of a parachute/payload system in which there is significant forward motion in addition to the descent.

**Gore** – the segment of a circular parachute canopy between the suspension lines.

**Guide Surface Parachute** – a type of solid textile parachute offering high stability, as measured by its angle of oscillation, but having a low drag coefficient.

**Heatshield** – the upstream facing portion of an aeroshell. The main role of the heatshield is to protect the payload from the heat of entry.

**Infinite-Mass Inflation** – an inflation of a parachute occurring such that the change in dynamic pressure is relatively modest during inflation. For a parachute, full inflation and the peak opening load will occur nearly simultaneously during an infinite-mass inflation. The term infinite-mass inflation arises from the observation that if a payload were to be of infinite mass (in a constant atmospheric density, gravity-free environment) the dynamic pressure would not vary during inflation since the drag of the parachute would be incapable of decelerating the payload. In practical situations infinite-mass inflations occur only when the payload is massive, and/or the atmospheric density is low, and/or in a wind tunnel.

**Inflatable Aerodynamic Decelerator** – a type of aerodynamic decelerator consisting of an inflatable structure that is either attached to the entry vehicle through one or more risers (trailing type) or is directly attached around the edges of the entry vehicle (attached type). The inflating fluid can be provided by either a gas generator or by capturing a portion of the airflow (i.e., ram-air). Inflatable aerodynamic decelerators are <u>not</u> intended to withstand the heat of entry. They are deployed and inflated at Mach numbers of five or less. See *ballute* and *inflatable aeroshell* for descriptions of related devices.

**Inflatable Aeroshell** – a type of aeroshell consisting of an inflatable structure directly attached around the edges of the payload to become part of the entry vehicle. Inflatable aeroshells are deployed and inflated (via one or more gas generators) before entry, and are intended to withstand the heat of entry. See *ballute* and *inflatable aerodynamic decelerator* for descriptions of related devices.

**Inflation** – the filling of a parachute with fluid. Inflation starts at the end of deployment and concludes with a fully filled parachute.

**Inflation Curve Method** – a method of calculating parachute opening loads that makes assumptions as to how the drag area of the parachute increases during inflation.

**Kaplun Number** – a nondimensional parameter expressing the ratio of material stiffness to fluid pressure forces.

**Lines-First Deployment** – a deployment procedure in which the bridles, risers, and suspension lines emerge from the deployment bag before the canopy.

**Mach Number** – the ratio of airspeed to the speed of sound of the fluid.

**Mortar** – a device used to eject a parachute at high speed from a vehicle to effect deployment.

**Nominal Area** – the constructed surface area of a parachute canopy including all openings such as the vent. Often used as a reference area for the aerodynamic coefficients of parachutes.

**Nominal Diameter** – a fictitious parachute diameter obtained by assuming that the nominal area of the parachute is that of a circle. Often used as a reference length for the aerodynamic coefficients of parachutes.

**Normal Force** – for a parachute, the component of aerodynamic force normal to its axis of symmetry.

**Normal Force Coefficient** – for a parachute, a nondimensional quantity defined as the normal force divided by the parachute's reference area and dynamic pressure.

**Opening Loads** - the forces generated by a parachute during inflation.

**Parafoil** – a non-circular gliding parachute whose shape resembles that of a wing.

**Peak Opening Load** – the largest force generated by a parachute during inflation.

**Permeability** – a measure of the amount of fluid that flows through a fabric.

**Pflanz's Method** - a simplified method of calculating a parachute's peak opening loads.

**Pilot Parachute** – a parachute used to deploy another parachute. The pilot parachute is usually smaller than the parachute it is deploying.

**Pitching Moment** – for a parachute, the aerodynamic moment normal to its axis of symmetry. The pitching moment is expressed about a given location, for example the parachute's suspension lines confluence point.

**Pitching Moment Coefficient** – for a parachute, a nondimensional quantity defined as the pitching moment divided by the parachute's reference area, reference length, and dynamic pressure. The pitching moment coefficient is expressed about a given location, for example the parachute's suspension lines confluence point.

**Projected Area** – the frontal area of a fully inflated parachute. Occasionally used as a reference area for the aerodynamic coefficients of parachutes.

**Projected Diameter** - a fictitious parachute diameter obtained by assuming that the projected area of the parachute is that of a circle. Occasionally used as a reference length for the aerodynamic coefficients of parachutes.

**Recoil Force** – the reaction force generated by a mortar while deploying a parachute.

**Reefing** – a method of parachute drag area and opening loads control during inflation. In a reefed parachute the skirt's inflated diameter is restricted by a reefing line threaded through a series of rings sewn along the skirt. To allow the parachute to reach full inflation the reefing line is severed by a reefing line cutter. Multiple stages of reefing can be used, thus controlling to some extent the inflation of the parachute.

**Reefing Line** – a braided cord threaded through a series of rings along the skirt of a parachute to restrict the skirt's inflated diameter and thus control drag and opening loads.

**Reefing Line Cutter** – a pyrotechnic device used to cut a reefing line. Reefing line cutters (typically 2 to 3 per reefing line) are usually sewn along the skirt of the parachute.

**Rigid Aerodynamic Decelerators** – a non-textile aerodynamic decelerator (e.g., drag ring, rotor).

**Ringsail Parachute** – a type of slotted textile parachute consisting of concentric fabric rings and sails (essentially rings with extra fullness) with gaps between them. Ringsail parachutes offer a good combination of drag and stability.

**Riser** – a single-leg textile component used to attach the parachute to the payload. Also, a textile component used to gather several suspension lines into a single leg.

**Sabot** – the piston that pushes the parachute out of a mortar. On one side of the sabot lies the parachute in its deployment bag, while on the other side the high-pressure gas created by the gas generator is pushing on the sabot.

**Skirt** – the upstream edge of a parachute canopy.

**Slotted Textile Parachutes** – a family of parachutes with concentric slots that allow air (or some other fluid) to flow through the canopy.

**Snatch Load** – the peak inertial load generated by a deploying parachute as it re-accelerates to the speed of the payload.

**Solid Textile Parachutes** – a family of parachutes whose canopies lack concentric openings (besides the vent) that allow air (or some other fluid) to flow through. Solid textile parachutes are usually manufactured using fabric materials.

**Static Aerodynamic Coefficients** – the aerodynamic coefficients of a body measured at a constant angle of attack with zero pitch and yaw rates.

**Suspension Lines** – braided cord connecting the skirt of the parachute to the payload.

**Suspension Lines Confluence Point** – a point in space where the suspension lines would theoretically come together if they were to continue upstream. In most parachutes the suspension lines are gathered by groups in risers – thus, the suspension lines often do not physically meet at the suspension lines confluence point. The suspension lines confluence point is useful as a reference point for the pitching moment.

**Tangential Force** – for a parachute, the component of aerodynamic force along its axis of symmetry.

**Tangential Force Coefficient** – for a parachute, a nondimensional quantity defined as the tangential force divided by the parachute's reference area and dynamic pressure.

**Textile Impact Attenuation Device** – an inflatable structure fabricated from textile materials and used to reduce the acceleration of a payload as it contacts the ground (e.g., airbags).

**Total Porosity** - the sum of the geometric porosity and an equivalent porosity due to fabric permeability. Fabric permeability (i.e., fluid flow through the fabric material) is converted to an "equivalent" open area of the parachute to determine the porosity due to fabric permeability.

**Trailing Distance** – the distance between the largest diameter of an entry vehicle and the skirt of the parachute.

**Trim Point/Angle of Attack** – the angle of attack at which the pitching moment of a parachute is zero.

**Tube** – the main cylindrical component of a mortar. The tube contains the parachute and its deployment bag and serves as the barrel through which the parachute (in its deployment bag) is accelerated by the sabot due to the fluid pressure created by the gas generator.

**Vent** – a circular opening at the apex of a parachute through which air (or some other fluid) flows.

**Vent Area** – the constructed area of the vent.

**Vent Diameter** – the diameter of a circular vent. Note that the vent area and vent diameter are not always related by the simple relationship between the area and diameter of a circle.

# Acknowledgements

**Pioneer Aerospace provided several of the photographs used in this presentation**

**Dr. Steve Lingard of Vorticity Ltd. provided the illustration of FSI**

# Point of Contact

**Juan R. Cruz**
**NASA Langley Research Center**
**Exploration Systems Engineering Branch**
**Mail Stop 489**
**Hampton, VA  23681**

**757-864-3173 (voice)**
**757-864-8675 (fax)**

**Juan.R.Cruz@NASA.GOV**

# Planetary Parachute Bibliography

Juan R. Cruz

NASA Langley Research Center
September 2005

**<u>Contents</u>**

---

[1] PEPP – Planetary Entry Parachute Program;  SPED – Supersonic Planetary Entry Decelerator Program; SHAPE – Supersonic High Altitude Parachute Experiment

# 1.0 Pre-Viking

## 1.1 General

1) Worth, R. N.: Maneuverable descent systems for Mars Landing, in: Proceedings of the Symposium on Manned Planetary Missions 1963/1964 Status, NASA-TM-X-53049, pp. 245-267, 1964.

2) Eckstrom, C. V.: Development and testing of the disk-gap-band parachute used for low dynamic pressure applications at ejection altitudes at or above 200,000 feet, NASA-CR-502, 1966.

3) Eckstrom, C. V.: Shaped parachute with stable flight characteristics, U. S. Patent 3,284,032, 1966.

4) Worth, R. N.: Descent and landing systems for unmanned Mars entry, *Journal of Spacecraft and Rockets*, Vol. 3, No. 12, pp. 1744-1748, 1966.

5) Barton, R. L.: Scale factors for parachute opening, NASA-TN-D-4123, 1967.

6) Heinrich, H. G.: Model laws governing parachute performance in Martian environment, *Wissenschaftliche Gesellschaft Fuer Luft – Und Raumfahrt and Deutsche Gesellschaft Fuer Raketentechnik Und Raumfahrt*, Vol. 11, Jul. – Sept., pp. 111-116, 1967.

7) Darnell, W. L., Henning, A. B., and Lundstrom, R. R.: A method for making large-scale decelerator tests in a simulated Mars environment, AIAA Paper 68-241, 1968

8) Gillis, C. L.: Aerodynamic decelerator systems for space missions, AIAA Paper 68-1081, 1968.

9) Guy, L. D.: Structural design options for planetary entry, AIAA Paper 68-344, 1968.

10) Harrison, E. F. and Slocumb, T. H.: Evaluation of entry and terminal deceleration systems for unmanned Martian landers, AIAA Paper 68-1147, 1968.

11) Moog, R. D.: Mars lander vehicle/parachute dynamics, in: Proceedings of the Fifth Space Congress, Vol. 2, pp. 10.2-1 – 10.2-30, 1968.

12) Murrow, H. N. and Preisser, J. S.: A method for controlling parachute deployment conditions in simulated planetary environments, NASA-TM-X-61215, 1968.

13) Zeiner, H., French, C., and Howard, D.: Evaluation of aerodynamic and propulsive terminal phase systems for an unmanned Mars soft lander, in: Proceedings of the Fifth Space Congress, Vol. 1, pp. 6.4-1 – 6.4-48, 1968.

14) Anon.: Titan/Mars hard lander, Volume I, 1400 lb capsule system design study, NASA-CR-66727-1, 1969.

15) Anon.: Titan/Mars hard lander, Volume II, Autonomous capsule system design study, NASA-CR-66727-2, 1969.

16) Gillis, C. L.: Deployable aerodynamic decelerators for space missions, *Journal of Spacecraft and Rockets*, Vol. 6, No. 8, pp. 885-890, 1969.

17) Faurote, G. L.: Design of disk-gap-band and modified ringsail parachutes and development of ballute apex inlet for supersonic application, NASA-CR-66909, 1970.

18) Ewing, E. G.: Deployable aerodynamic deceleration systems, NASA space vehicle design criteria (structures), NASA-SP-8066, 1971.

## 1.2  Wind Tunnel Testing

19) Maynard, J. D.: Aerodynamic characteristics of parachutes at Mach numbers from 1.6 to 3.0, NASA-TN-D-752, 1961.

20) Galigher, L. L.: Aerodynamic characteristics of ballutes and disk-gap-band parachutes at Mach numbers from 1.8 to 3.7, AEDC-TR-69-245, 1969.

21) Whitlock, C. H.: Wind tunnel investigation of inflation of disk-gap-band and modified ringsail parachutes at dynamic pressures between 0.24 and 7.07 pounds per square foot, NASA-TM-X-1786, 1969.

22) Bobbitt, P. J. and Mayhue, R. J.: Supersonic and subsonic wind-tunnel tests of reefed and unreefed disk-gap-band parachutes, AIAA Paper 70-1172, 1970.

23) Mayhue, R. J. and Bobbitt, P. J.: Drag characteristics of a disk-gap-band parachute with a nominal diameter of 1.65 meters at Mach numbers from 2.0 to 3.0, NASA-TN-D-6894, 1972.

24) Couch, L. M.: Drag and stability characteristics of a variety of reefed and unreefed parachute configurations at Mach 1.80 with an empirical correlation for subsonic Mach numbers, NASA-TR-R-429, 1975.

## 1.3 Flight Test Programs (PEPP, SPED, SHAPE and Others)

25) Whitlock, C. H. and Murrow, H. N.: Performance characteristics of a preformed elliptical parachute at altitudes between 200,000 and 100,000 feet obtained by in-flight photography, NASA-TN-D-2183, 1964.

26) Boettcher, E. W.: Planetary Entry Parachute Program, cross parachute engineering design report, NASA-CR-66590, 1967.

27) Eckstrom, C. V. and Murrow, H. N.: Flight test of a 40-foot-nominal-diameter modified ringsail parachute deployed at a Mach number of 1.64 and a dynamic pressure of 9.1 pounds per square foot, NASA-TM-X-1484, 1967. (Film supplement L-981 available from the NASA LaRC Library.)

28) Eckstrom, C. V. and Preisser, J. S.: Flight test of a 30-foot-nominal-diameter disk-gap-band parachute deployed at a Mach number of 1.56 and a dynamic pressure of 11.4 pounds per square foot, NASA-TM-X-1451, 1967. (Film supplement L-968 available from the NASA LaRC Library.)

29) Darnell, W. L., Henning, A. B., and Lundstrom, R. R.: Flight test of a 15-foot-diameter (4.6 meter) 120° conical spacecraft simulating parachute deployment in a Mars atmosphere, NASA-TN-D-4266, 1967.

30) Lemke, R. A.: Final report: 40 ft DGB parachute, NASA-CR-66587, 1967.

31) Lemke, R. A., Moroney, R. D., Neuhaus, T. J., and Niccum, R. J.: Design report, 65 foot diameter D-G-B parachute, Planetary Entry Parachute Program, NASA-CR-66589, 1967.

32) McFall, J. C. and Murrow Jr., H. N.: Parachute testing at altitudes between 30 and 90 kilometers, *Journal of Spacecraft and Rockets*, Vol. 4, June, pp. 796-798, 1967.

33) Preisser, J. S. and Eckstrom, C. V.: Flight Test of a 31.2-foot-diameter modified ringsail parachute deployed at a Mach number of 1.39 and a dynamic pressure of 11.0 pounds per square foot, NASA-TM-X-1414, 1967. (Film supplement L-966 available from the NASA LaRC Library.)

34) Stone, F. J.: Final technical report, 55-ft-$D_0$ ringsail parachute, Planetary Entry Parachute Program, NASA-CR-66588, 1967.

35) Whitlock, C. H., Bendura, R. J., and Coltrane, L. C.: Performance of a 26-meter-diameter ringsail parachute in a simulated Martian environment, NASA-TM-X-1356, 1967. (Film supplement L-946 available from the NASA LaRC Library.)

36) Bendura, R. J., Huckins III, E. K., and Coltrane, L. C.: Performance of a 19.7-meter-diameter disk-gap-band parachute in a simulated Martian environment, NASA-TM-X-1499, 1968. (Film supplement L-983 available from the NASA LaRC Library.)

37) Eckstrom, C. V. and Preisser, J. S.: Flight test of a 40-foot-nominal-diameter disk-gap-band parachute deployed at a Mach number of 2.72 and a dynamic pressure of 9.7 pounds per square foot, NASA-TM-X-1623, 1968. (Film supplementL-1006 available from the NASA LaRC Library.)

38) Gillis, C. L and Bendura, R. J.: Full-scale simulation of parachute deployment environment in the atmosphere of Mars, in: Proceedings of the 14th Annual Technical Meeting, Institute Environ. Sci., 1968, pp. 469-475.

39) Lundstrom, R. R., Darnell, W. L., and Coltrane, L. C.: Performance of a 16.6-meter-diameter cross parachute in a simulated Martian environment, NASA-TM-1543, 1968. (Film supplement L-985 available from the NASA LaRC Library.)

40) McFall, J. C. and Murrow Jr., H. N.: Summary of experimental results obtained from the NASA Planetary Entry Parachute Program, AIAA Paper 68-934, 1968.

41) Preisser, J. S. and Eckstrom, C. V.: Flight test of a 30-foot-nominal-diameter cross parachute deployed at a Mach number of 1.57 and a dynamic pressure of 9.7 pounds per square foot, NASA-TM-X-1542, 1968. (Film supplement L-994 available from the NASA LaRC Library.)

42) Preisser, J. S. and Eckstrom, C. V.: Flight test of a 40-foot-nominal-diameter disk-gap-band parachute deployed at a Mach number of 1.91 and a dynamic pressure of 11.6 pounds per square foot, NASA-TM-X-1575, 1968. (Film supplement L-1000 available from the NASA LaRC Library.)

43) Whitlock, C. H., Henning, A. B., and Coltrane, L. C.: Performance of a 16.6-meter-diameter modified ringsail parachute in a simulated Martian environment, NASA-TM-X-1500, 1968. (Film supplement L-984 available from the NASA LaRC Library.)

44) Murrow, H. N. and McFall Jr., J. C.: Some test results from the NASA Planetary Entry Parachute Program, *Journal of Spacecraft*, Vol. 6, No. 5, pp. 621-623, 1969.

45) Whitlock, C. H. and Bendura, R. J.: Inflation and performance of three parachute configurations from supersonic flight tests in a low-density environment, NASA-TN-D-5296, 1969.

46) Eckstrom, C. V.:  High-altitude flight test of a 40-foot-diameter (12.2-meter) ringsail parachute at a deployment Mach number of 2.95, NASA-TN-D-5796, 1970. (Film supplement L-1077 available from the NASA LaRC Library.)

47) Eckstrom, C. V.:  Flight test of a 40-foot-nominal-diameter disk-gap-band parachute deployed at a Mach number of 3.31 and a dynamic pressure of 10.6 pounds per square foot, NASA-TM-X-1924, 1970.  (Film supplement L-1066 available from the NASA LaRC Library.)

48) Murrow, H. N. and Eckstrom, C. V.:  Low- and high-altitude tests of parachutes designed for use in low-density atmospheres, AIAA Paper 70-1164, 1970.

49) Eckstrom, C. V. and Murrow, H. N.:  Flight tests of cross, modified ringsail, and disk-gap-band parachutes from a deployment altitude of 3.05 km (10 000 ft), NASA-TM-X-2221, 1971.

50) Preisser, J. S. and Grow, R. B.:  High-altitude flight test of a reefed 12.2-meter-diameter disk-gap-band parachute with deployment at a Mach number of 2.58, NASA-TN-D-6469, 1971.  (Film supplement L-1106 available from the NASA LaRC Library.)

51) Eckstrom, C. V. and Branscome, D. R.:  High-altitude flight test of a disk-gap-band parachute deployed behind a bluff body at a Mach number of 2.69, NASA-TM-X-2671, 1972.

52) Henning, A. B. and Lundstrom, R. R.:  Flight test of an erectable spacecraft used for decelerator testing at simulated Mars entry conditions, NASA-TN-D-6910, 1972.

# 2.0  Viking

## 2.1  General

53) Lau, R. A. and Hussong, J. C.:  The Viking Mars lander decelerator system, AIAA Paper 70-1162, 1970.

54) Gillis, C. L.:  The Viking decelerator system – An overview, AIAA Paper 73-442, 1973.

55) Houmard, J. E.:  Stress analysis of the Viking parachute, AIAA Paper 73-444, 1973.

56) Hopper, F. W.:  Trajectory, atmosphere, and wind reconstruction from Viking entry measurements, AAS 75-068, 1975.

57) Ingoldby, R. N., Michel, F. C., Flaherty, T. M., Doty, M. G., Preston, B., Villyard, K. W., and Steele, R. D.: Entry data analysis for Viking landers 1 and 2 – Final Report, NASA-CR-159388, 1976.

58) Martin Marietta Corp.: Viking lander "as built" performance capabilities, Martin Marietta Corp. Report, NASA Contract NAS1-9000, 1976.

59) Seiff, A.: Mars atmospheric winds indicated by motion of the Viking landers during parachute descent, *Journal of Geophysical Research*, Vol. 98, No. E4, pp. 7461-7474, 1993.

## 2.2  Wind Tunnel Testing

60) Jaremenko, I., Steinberg, S., and Faye-Petersen, R.: Scale model test results of the Viking parachute system at Mach numbers from 0.1 through 2.6, NASA-CR-149377, 1971.

61) Reichenau, D. E. A.: Aerodynamic Characteristics of disk-gap-band parachutes in the wake of Viking entry forebodies at Mach numbers from 0.2 to 2.6, AEDC-TR-72-78, 1972.

62) Steinberg, S. Siemers III, P. M., and Slayman, R. G.: Development of the Viking parachute configuration by wind-tunnel investigation, *Journal of Spacecraft*, Vol. 11, No. 2, pp. 101-107, 1974.  (Also available as AIAA Paper 73-545, 1973.)

63) Foughner, J. T.: Viking Mars mission support investigations in the Langley transonic dynamics tunnel, NASA-TM-80234, 1980.

## 2.3  Low Altitude Drop Tests (LADT)

64) Murrow, H. N., Eckstrom, C. V., and Henke, D. W.: Development flight tests of the Viking decelerator system, AIAA Paper 73-455, 1973.

## 2.4  Balloon Launched Decelerator Tests (BLDT)

65) Dickinson, D., Schlemmer, J., Hicks, F., Michel, F., and Moog, R. D.: Balloon Launched Decelerator Test program, Post-flight test report, BLDT vehicle AV-1, NASA-CR-112176, 1972.

66) Dickinson, D., Schlemmer, J., Hicks, F., Michel, F., and Moog, R. D.: Balloon Launched Decelerator Test program, Post-flight test report, BLDT vehicle AV-2, NASA-CR-112177, 1972.

67) Dickinson, D., Schlemmer, J., Hicks, F., Michel, F., and Moog, R. D.: Balloon Launched Decelerator Test program, Post-flight test report, BLDT vehicle AV-4, NASA-CR-112179, 1972.

68) Dickinson, D., Schlemmer, J., Hicks, F., Michel, F., and Moog, R. D.: Balloon Launched Decelerator Test program, Post-flight test report, BLDT vehicle AV-3, NASA-CR-112178, 1973.

69) Moog, R. D., Bendura, R. J., Timmons, J. D., and Lau, R. A.: Qualification flight tests of the Viking decelerator system, AIAA Paper 73-457, 1973.

70) Moog, R. D. and Michel, F. C.: Balloon launched Viking decelerator test program summary report, NASA-CR-112288, 1973.

71) Raper, J. L., Lundstrom, R. R., and Michel, F. C.: The Viking parachute qualification test technique, AIAA Paper 73-456, 1973.

72) Bendura, R. J., Lundstrom, R. R., Renfroe, P. G., and LeCroy, S. R.: Flight tests of Viking parachute system in three Mach number regimes, Part II – Parachute test results, NASA-TN-D-7734, 1974.

73) Buna, T. and Battley, H. H.: Thermal design and performance of the Viking balloon-launched decelerator test vehicles, AIAA Paper 74-760, 1974.

74) Lundstrom, R. R., Raper, J. L., Bendura, R. J., and Shields, E. W.: Flight tests of Viking parachute system in three Mach number regimes, Part I – Vehicle description, test operations, and performance, NASA-TND-7692, 1974.

75) Moog, R. D., Bendura, R. J., Timmons, J. D., and Lau, R. A.: Qualification tests of the Viking decelerator system, *Journal of Spacecraft*, Vol. 11, No. 3, pp. 188-195, 1974.

76) Shields, E. W.: Statistical Trajectory Estimation Program (STEP) implementation for BLDT post flight trajectory simulation, NASA CR-132427, 1974.

77) Timmons, J. D.: Viking balloon launched decelerator test, IAF Paper IAF-76-155, 1976.

## 2.5  Mortar Testing and Qualification

78) Brecht, J. P., Pleasants, J. E., and Mehring, R. D.: The Viking mortar: Design, development, and flight qualification, AIAA Paper 73-458, 1973.

## 2.6  Multi-Body Dynamic Analyses

79)  Whitlock, C. H., Poole, L. R., and Talay, T. A.:  Postflight simulation of parachute deployment dynamics of Viking qualification flight tests, NASA-TN-D-7415, 1973.

80)  Talay, T. A.:  Parachute-deployment-parameter identification based on an analytical simulation of Viking BLDT AV-4, NASA-TN-D-7678, 1974.

# 3.0  Mars Pathfinder

81)  Fallon II, E. J.:  System design overview of the Mars Pathfinder parachute decelerator subsystem, AIAA Paper 97-1511, 1997.

82)  Peng, C.-Y., Tsang, S. K., Smith, K., Sabahi, D., Short, K., and Mauritz, A.:  Model correlation for Mars Pathfinder entry, descent and landing simulation, in: Proceedings of the 1997 IEEE Aerospace Conference, Vol. 1, pp. 233-246, 1997.

83)  Spencer, D. A., Blanchard, R. C., Thurman, S. W., Braun, R. D., Peng, C.-Y., and Kallemeyn Jr., P. H.:  Mars Pathfinder atmospheric entry reconstruction, *Advances in Astronautical Sciences*, Vol. 99, Pt. 1, pp. 663-692, 1998.  (Also available as AAS Paper 98-146, 1998.)

84)  Braun, R. D., Spencer, D. A., Kallemeyn, P. H., and Vaughan, R. M.:  Mars Pathfinder atmospheric entry navigation operations, *Journal of Spacecraft and Rockets*, Vol. 36, No. 3, pp. 348-356, 1999.  (Also available as AIAA Paper 97-3663, 1997.)

85)  Spencer, D. A., Blanchard, R. C., Braun, R. D., Kallemeyn, P. H., and Thurman, S. W.:  Mars Pathfinder entry, descent, and landing reconstruction, *Journal of Spacecraft and Rockets*, Vol. 36, No. 3, pp. 357-366, 1999.

86)  Witkowski, A.:  Mars Pathfinder parachute system performance, AIAA Paper 99-1701, 1999.

87)  Desai, P. N., Schofield, J. T., and Lisano, M. E.:  Flight reconstruction of the Mars Pathfinder disk-gap-band parachute drag coefficient, AIAA Paper 2003-2126, 2003.

# 4.0  Mars Exploration Rover

## 4.1  General

88)  Mitcheltree, R. A.:  Dynamic scaling for Earth based testing of Mars terminal descent dynamics, AIAA Paper 2003-5391, 2003.

89) Steltzner, A., Cruz, J., Bruno, R., and Mitcheltree, R.: Opportunities and limitations in low Earth subsonic testing for qualification of extraterrestrial supersonic parachute designs, AIAA Paper 2003-2135, 2003.

90) Steltzner, A., Desai, P., Lee, W., and Bruno, R.: The Mars Exploration Rovers entry descent and landing and the use of aerodynamic decelerators, AIAA Paper 2003-2125, 2003.

91) Witkowski, A. and Bruno, R.: Mars Exploration Rover parachute decelerator system program overview, AIAA Paper 2003-2100, 2003.

92) Desai, P. N. and Knocke, P. C.: Mars Exploration Rovers entry, descent, and landing trajectory analysis, AIAA Paper 2004-5092, 2004.

93) Raiszadeh, B. and Queen, E. M.: Mars Exploration Rover terminal descent mission modeling and simulation, AAS 04-271, 2004.

94) Witkowski, A., Kandis, M., Bruno, R., and Cruz, J. R.: Mars Exploration Rover parachute system performance, AIAA Paper 2005-1605, 2005.

## 4.2   Wind Tunnel Testing

95) Cruz, J. R., Kandis, M., and Witkowski, A.: Opening loads analyses for various disk-gap-band parachutes, AIAA Paper 2003-2131, 2003.

96) Cruz, J. R., Mineck, R. E., Keller, D. F., and Bobskill, M. V.: Wind tunnel testing of various disk-gap-band parachutes, AIAA Paper 2003-2129, 2003.

97) Zell, P. T., Cruz, J. R., and Witkowski, A.: Structural testing of parachutes in the National Full-Scale Aerodynamics Complex 80-by-120-foot wind tunnel at NASA Ames Research Center, AIAA Paper 2003-2130, 2003.

98) Schoenenberger, M., Queen, E. M., and Cruz, J. R.: Parachute aerodynamics from video data, AIAA Paper 2005-1633, 2005.

## 4.3   Low Altitude Drop Tests

99) Taeger, Y. and Witkowski, A.: A summary of dynamic testing of the Mars Exploration Rover parachute decelerator system, AIAA Paper 2003-2127, 2003.

100) Way, D. W., Desai, P. N., Engelund, W. C., Cruz, J. R., and Hughes, S. J.: Design and analysis of the drop test vehicle for the Mars Exploration Rover parachute structural tests, AIAA Paper 2003-2128, 2003.

### 4.4   Mortar Testing and Qualification

101) Vasas, R. E. and Styner, J.:  Mars Exploration Rover parachute mortar deployer development, AIAA Paper 2003-2137, 2003.

# 5.0   Pioneer/Venus, Galileo, Beagle 2, Genesis, Cassini/Huygens, Stardust, and Mars Science Laboratory

102) Nolte, L. J. et al.:  Final report:  System design of the Pioneer Venus spacecraft – Volume 5:  Probe vehicle studies, NASA-CR-137492, 1973.

103) Nolte, L. J. and Sommer, S. C.:  Probing a planetary atmosphere:  Pioneer Venus spacecraft description, AIAA Paper 75-1160, 1975.

104) Talley, R. G.:  Pioneer Venus deceleration module final report, General Electric Re-entry & Environmental Systems Division, 1978.

105) Rodier, R. W., Thuss, R. J., and Terhune, J. E.:  Parachute design for the Galileo Jupiter entry probe, AIAA Paper 81-1951, 1981.

106) Corridan, R., Givens, J., and Kepley, B.:  Transonic wind tunnel investigation of the Galileo probe parachute configuration, AIAA Paper 84-0823, 1984.

107) McMenamin, H. J. and Pochettino, L. R.:  Galileo parachute system modification program, AIAA Paper 84-0824CP, 1984.

108) Achtermann, Kapp, R., and Lehra, H.:  Parachute characteristics of Titan descent modules planetary probe, BF-3/86-B/ESA-CR(P)-2438, 1986.

109) Lingard, J. S. and Underwood, J. C.:  Wind tunnel testing of disk-gap-band parachutes related to the Cassini-Huygens mission, AIAA Paper 93-1200, 1993.

110) Lorenz, R. D.:  Scientific implications of the Huygens Parachute System, AIAA Paper 93-1215, 1993.

111) Lingard, J. and Underwood, J.:  The effect of low density atmospheres on the aerodynamic coefficients of parachutes, AIAA Paper 95-1556, 1995.

112) Neal, M. F. and Wellings, P. J.:  Design and qualification of the descent control sub-system for the Huygens probe, AIAA Paper 95-1533, 1995.

113) Underwood, J.:  Development testing of disk-gap-band parachutes for the Huygens probe, AIAA Paper 95-1549, 1995.

114) McMenamin, H. J.: Galileo parachute system performance, AIAA Paper 97-1510, 1997.

115) Underwood, J. C.: A system drop test of the Huygens probe, AIAA Paper 97-1429, 1997.

116) Underwood, J. C. and Sinclair, R. J.: Wind tunnel testing of parachutes for the Huygens probe, in: Wind Tunnels and Wind Tunnel Test Techniques, pp. 47.1–47.11, The Royal Aeronautical Society, 1997.

117) Witkowski, A.: The Stardust sample return capsule parachute recovery system, AIAA Paper 99-1741, 1999.

118) Brown, G., Haggard, R., and Corwin, R. A.: Parafoil mid-air retrieval for space sample return missions, AIAA Paper-2001-0218, 2001.

119) Fallon II, E. J. and Sinclair, R.: Design and development of the main parachute for the Beagle 2 Mars lander, AIAA Paper 2003-2153, 2003.

120) Haigh, A.: Five month program for the new main parachute for the Beagle 2 Mars lander, AIAA Paper 2003-2170, 2003.

121) Northey, D.: The main parachute for the Beagle 2 Mars lander, AIAA Paper 2003-2171, 2003.

122) Witkowski, A., Machalick, W., and Taeger, Y.: Mars subsonic parachute technology task system overview, AIAA Paper 2005-1657, 2005.

123) Mitcheltree, R., Bruno, R., Slimko, E., Baffes, C., Konefat, E., and Witkowski, A.: High altitude test program for a Mars subsonic parachute, AIAA Paper 2005-1659, 2005.

## 6.0  Other

124) Alexander, W. C. and Foughner Jr., J. T.: Drag and stability characteristics of high-speed parachutes in the transonic range, AIAA Paper 73-473, 1973.

125) Foughner Jr., J. T. and Alexander, W. C.: Wind tunnel tests of modified cross, hemisflo, and disk-gap-band parachutes with emphasis in the transonic range, NASA-TN-D-7759, 1974.

126) Anon.: Study of advanced atmospheric entry systems for Mars, Final report, NASA-CR-157548, 1978.

127) Eiden, M. J.: Aerodynamic decelerators for future European space missions, AIAA Paper 89-0879, 1989.

128) Ludtke, W. P.: Wind tunnel tests of a 20-gore disk-gap-band parachute, NSWC TR 89 180, 1989.

129) Ravnitzky, M. J., Patel, S. N., and Lawrence, R. A.: To fall from space: Parachutes and the space program, AIAA Paper 89-0926, 1989.

130) Raiszadeh, B. and Queen, E. M.: Partial validation of multibody Program to Optimize Simulated Trajectories II (POST II) parachute simulation with interacting forces, NASA-TM-2002-211634, 2002.

131) Masciarelli, J. P., Cruz, J. R., and Hengel, J. E.: Development of an improved performance parachute system for Mars missions, AIAA Paper 2003-2138, 2003.

132) Raiszadeh, B.: Multibody parachute flight simulations for planetary entry trajectories using "equilibrium points," AAS 03-163, 2003.

133) Lingard, J. S. and Darley, M. G.: Simulation of parachute fluid structure interaction in supersonic flow, AIAA Paper 2005-1607, 2005.

134) Manning, R. M. and Adler, M.: Landing on Mars, AIAA Paper 2005-6742, 2005.

Notes

Notes

Notes

Notes